ABSTRACT

DUBOSCQ, SANDRINE MARIE. $^{3}H/^{3}He$ Groundwater Ages and Discharge of Per- and Polyfluoroalkyl Substances from Groundwater to a Stream near the Chemours Company in Bladen County, North Carolina (Under the direction of Dr. David P. Genereux).

Per- and polyfluoroalkyl substances (PFAS) are manmade chemicals that are highly persistent, bioaccumulative and toxic. In North Carolina, PFAS have been released from the chemical plant on the Fayetteville Works property near Fayetteville, NC through air emissions and process wastewater starting sometime between 1971 and 1980. The deposition on the ground surface of PFAS from air emissions over the past 40 to 50 years has caused extensive contamination of surface water and groundwater in the area.

In this work, groundwater sampling and water flux measurements were carried out at 24 different points in the streambed of Georgia Branch, a tributary of the Cape Fear River near the Fayetteville Works, on February 25th and 26th, 2019. Groundwater from each point was sampled for 27 PFAS compounds and to determine age by tritium-helium age dating. The age of groundwater discharging was coupled with groundwater flux and PFAS concentrations in order to understand the relationship between PFAS concentration and age of groundwater and to assess the transit time of groundwater and PFAS in the surficial aquifer.

At each streambed measurement point, water flux through the streambed was upward from groundwater to the stream; the mean specific discharge was 1.53 m day^{-1} (standard deviation 1.19 m day^{-1}). Mean total PFAS concentration of groundwater at all 24 points was 2039 ng L^{-1} (s.d. = 1001 ng L^{-1}). Mean total PFAS flux from groundwater to the Georgia Branch stream was 2.90 mg m^{-2} d^{-1} (s.d. = 2.69 mg m^{-2} d^{-1}) and mean GenX flux was 0.72 mg m^{-2} d^{-1} (s.d. = 0.96 mg m^{-2} d^{-1}). Only 4 of the 24 sampled points had GenX concentrations below North Carolina's drinking water health goal for GenX of 140 ng L^{-1}.

Tritium-helium age dating of streambed groundwater suggested that the groundwater discharging into Georgia Branch had predominantly very young apparent ages; 21 of 24 points had ages of 0 to 5 years. Estimated ages at the other three points were 14, 18, and 28 years. The predominance of groundwater with young apparent ages is unusual compared to the distribution of ages from similar studies in the North Carolina coastal plain and in Wisconsin (Browne and Guldan, 2005; Kennedy et al., 2009a,b; Gilmore et al., 2016a). A general pattern of decreasing PFAS concentration with increasing tritium-helium age was observed, but with a wide range of PFAS concentrations in the 21 samples with very young apparent age (0-5 years).

Four different hydrogeological mechanisms were identified as potential causes of the high proportion of very young tritium-helium ages in groundwater discharging to Georgia Branch: hyporheic flow, diffusive fractionation of ^{3}He, low recharge rate, and riparian re-infiltration of exfiltrated groundwater. The latter two mechanisms seem the most plausible at Georgia Branch. The low recharge rate mechanism would suggest that the very young tritium-helium apparent ages are affected by loss of ^{3}He and may not be fully accurate. The re-infiltration mechanism would suggest that the very young ages are true age dates, for the short flowpath of groundwater from the riparian areas to the streambed after re-infiltration rather than from the location of initial recharge to the streambed.

The results of this study show that PFAS concentrations were generally lower in the older groundwater. These results are consistent with other data collected at Georgia Branch and nearby tributaries to the Cape Fear River where no samples without PFAS have been found, suggesting that the time for PFAS to be transported through the surficial aquifer must be shorter than the time PFAS have been produced in the area, i.e., fewer than 48 years at most for samples collected in 2019.

© Copyright 2020 by Sandrine Duboscq

All Rights Reserved

$^{3}H/^{3}He$ Groundwater Ages and Discharge of Per- and Polyfluoroalkyl Substances from Groundwater to a Stream near the Chemours Company in Bladen County, North Carolina

by
Sandrine Marie Duboscq

A thesis submitted to the Graduate Faculty of
North Carolina State University
in partial fulfillment of the
requirements for the degree of
Master of Science

Marine, Earth, and Atmospheric Sciences

Raleigh, North Carolina
2020

APPROVED BY:

_____	_____
Dr. David Genereux Committee Chair	Dr. Detlef Knappe

_____
Dr. Helena Mitasova

DEDICATION

In dedication to my father, Jean Etienne Duboscq, who first attempted to teach me logarithms in kindergarten; and to my mother, Catherine J. Lance, who has shown me how to live a life of constant learning.

BIOGRAPHY

Sandrine Duboscq was born and raised in Ithaca, NY. She earned her B.S. in Geological Sciences from the University at Buffalo, along with minors in Geographic Information Systems and French Language and Literature, in May 2018.

ACKNOWLEDGMENTS

I would like to thank my advisor, Dr. David Genereux, for the guidance and advice, and the many, many drafts revised. I am very grateful to my committee members, Dr. Detlef Knappe and Dr. Helena Mitasova, for the time they have taken to support this work and for their expertise in guiding this project. I would like to acknowledge the support by Dr. Troy E. Gilmore in the field during data collection and guidance during data interpretation. I would like to express my gratitude to Dr. D. Kip Solomon at the University of Utah for sharing his expertise in groundwater age dating, and Dr. Solomon and his lab, the Dissolved and Noble Gas Laboratory, for groundwater age dating analysis. I would like to thank Dr. Detlef Knappe and his Water Quality and Treatment Research Group, including Zachary Hopkins, for the extensive analysis of PFAS in my groundwater samples. I thank Stacie Reckling and Blake Baines for their data and field support, and I would also like to thank Lydia Koropeckyj-Cox and Dr. Marie-Amélie Pétré for their continuous encouragement and support during this project. I gratefully acknowledge the financial support of this project by the North Carolina Policy Collaboratory through awards to Dr. D.P. Genereux, Dr. D.R.U. Knappe, and Dr. T.E. Gilmore. Finally, I would like to thank my mother, Catherine Lance, my stepfather, Chris Dilger, and the rest of my wonderful support network, including my family, friends, and my partner, for their constant love and understanding along the way.

TABLE OF CONTENTS

LIST OF TABLES vi
LIST OF FIGURES vii

1. Introduction 1
2. Background on PFAS **3**
2.1. Structure and properties of PFAS 3
2.2. GenX and HFPO-DA 3
2.3. Background of GenX and other PFAS at the study site 6
3. Background on tritium-helium age dating **8**
4. Study Area **9**
4.1. Coastal Plain hydrogeology 9
4.2. Local geology 9
4.3. Climate 12
4.4. Land and water use 12
5. Study design **13**
6. Methods **14**
6.1. Specific discharge 14
6.2. PFAS flux and concentration 16
6.3. Groundwater age dating 18
7. Results **18**
7.1. Water flux 18
7.2. PFAS concentration and flux 22
7.3. Tritium-helium groundwater age dating results 33
7.4. Concentration of PFAS and age of groundwater 36
7.5. PFAS transit time distribution 47
8. Mechanisms that may affect tritium-helium age dating **49**
8.1. The age dating puzzle 49
8.2. Sampling errors 49
8.3. Sampling in the hyporheic zone 50
8.4. Diffusive fractionation of ^{3}H and tritiogenic ^{3}He 51
8.5. The Low Recharge Rate Mechanism: Loss of tritiogenic ^{3}He at the water table due to low recharge rate 52
8.6. The Re-infiltration Mechanism: Re-infiltration of groundwater exfiltrated from the perched saturated zone 54
8.7. Interpretation of *TTD* mechanisms 55
9. Summary and Conclusions **59**
9.1. Future Work 61
REFERENCES **63**
APPENDICES **69**
APPENDIX A. Tritium-Helium Age Dating Results and Noble Gas Analysis **70**

LIST OF TABLES

Table 1. The molecular formulas and structures of GenX and HFPO-DA and their common anion when in water. Molecular images are from the EPA Comptox Database (Comptox, 2019) 5

Table 2. The PFAS compounds for which the groundwater samples were analyzed, their acronyms, and molecular formulas 16

Table 3. Comparison of results on streambed *v*, *K*, and *J* between the present study and 4 other studies of streambeds in the North Carolina Coastal Plain 20

Table 4. Vertical water flux (*v*), hydraulic conductivity (*K*), and vertical hydraulic head gradient (*J*) for each streambed measurement point in Georgia Branch, 25-26 February 2019. Each point is named by its distance downstream along the channel in meters from the zero point established just east of Glengerry Road in October 2018, and whether it was on the left side, center, or right side of the streambed (L, C, or R, respectively), from the perspective of an observer facing downstream. 21

Table 5. PFAS concentrations in groundwater at 24 points in/beneath the streambed of Georgia Branch and one surface water sample (GB387 SW). When the concentration was lower than the minimum reporting level (<5 ng L^{-1}), it was considered zero in calculations of total measured PFAS and average concentration of each PFAS. Two ** after a concentration represents a concentration that was above the highest calibration curve point and one * represents a sample injection where the peak area fell outside of the analytical window for that compound on the LC/MS and no concentration was reported by the lab. 26

Table 6. Streambed flux (groundwater to stream) of the 10 PFAS compounds present in groundwater samples, and total PFAS flux, in mg m^{-2} d^{-1}, at 24 points in the streambed of Georgia Branch, February 2019 31

Table 7. The mean (μ), standard deviation (σ), and the coefficient of variation of PFAS concentration and flux of the 8 most abundant PFAS. 33

Table 8. Log K_{oc} values found by Geosyntec (2019b) using a linear free energy relationship between K_{ow} and K_{oc}, and experimental values of K_{ow}. Also shown are the estimated retardation factors of the eight most abundant PFAS at the study site 39

LIST OF FIGURES

Figure 1. 11 NCDEQ boreholes where borehole stratigraphy has been measured (NCDEQ 2019a). NHD refers to the USGS's National Hydrography Dataset. The name of each borehole is shown in a white box on the map. The base map was created using shapefiles provided by the USGS (USGS Map, 2016a-l) 10

Figure 2. Hydrostratigraphy of the 11 boreholes shown in Fig. 2, ordered from west, on the left, to east, on the right (NCDEQ, 2019a). The bottom of each column represents the bottom of the borehole, not necessarily the bottom of the deepest layer shown. The average stratigraphic thickness of the surficial aquifer in this area is 15.9 m..... 11

Figure 3. The saturated thickness of the surficial aquifer at the DuPont Corporation well, located at the Chemours Company (Figs. 1, 2), as monitored by the NC Department of Environmental Quality's Division of Water Quality from April 4, 2004 to February 3, 2019 (NCDEQ, 2019b). Mean saturated thickness from 2004 to 2019, 14 m, is indicated by the blue line..... 12

Figure 4. Left image shows the locations of the Fayetteville Works and the Georgia Branch watershed. On the right, the Georgia Branch streambed sampling points are labeled on a Digital Elevation Model (DEM). Data for the delineation of the Georgia Branch watershed comes from the 1-meter DEMs provided by the USGS, NHD refers to the USGS's National Hydrography Dataset (USGS Map, 2017). The left base map is modified from the USGS Topo Map Data and Topo Style Sheet, downloaded from the National Map (USGS Map, 2016a,b). The close up of Georgia Branch was defined by Blake Baines from NCSU using LiDAR data provided by North Carolina's SPtaial Data Download and displayed by M.A. Pétré on a DEM from the USGS (USGS Map, 2017; USGS, 2016d) 15

Figure 5. The relationship between hydraulic conductivity, *K*, and specific discharge, *v*, in the streambed of Georgia Branch in February 2019 19

Figure 6. Water flux (specific discharge, *v*) through the streambed of Georgia Branch, 25-26 February 2019. Blue, gray, and orange bars show streambed sampling points on the right side, center, and left side of the channel, respectively. Three point transects across the channel were sampled at 330 m, 387 m, 412 m, 450 m, and 490 m. A point on the left side of the channel was not feasible at the 490 m transect, but measurements were made at 487L, and the water flux at 487L is plotted above as part of the 490 m transect 22

Figure 7. Total PFAS concentrations in groundwater at 24 points in/beneath the streambed of Georgia Branch. At each 3-point transect across the stream, the group of three bars shows, from left to right, the total PFAS concentrations at the left, center and right points. A point on the left side of the channel was not feasible at the 490 m transect, but measurements were made at 487L, and the PFAS data at 487L are plotted above as part of the 490 m transect 25

Figure 8. PFAS flux at 24 points in the streambed of Georgia Branch, February 2019. At each 3-point transect, the group of three bars shows, from left to right, the PFAS flux values at the left, center and right points. The 7 PFAS compounds shown make up 99.4% of the PFAS flux in Georgia Branch groundwater samples from February 2019. On average, PMPA, GenX, PFO2HxA, and PEPA together make up 93.3% of total PFAS flux 30

Figure 9. The transit time distribution of groundwater discharging at 24 points in the Georgia Branch stream channel. All of the discharge associated with the 21 streambed points with very young apparent age (0-5 years) was summed and plotted at zero transit time 36

Figure 10. The relationship between total PFAS concentration and groundwater age at 24 points in Georgia Branch. Groundwater samples of very young apparent age (0-5 years), and stream water from GB387, are plotted at zero age 40

Figure 11. The relationship between PMPA concentration and groundwater age at 24 points in Georgia Branch. Groundwater samples of very young apparent age (0-5 years), and stream water from GB387, are plotted at zero age 41

Figure 12. The relationship between GenX concentration and groundwater age at 24 points in Georgia Branch. Groundwater samples of very young apparent age (0-5 years), and stream water from GB387, are plotted at zero age 41

Figure 13. The relationship between PFO2HxA concentration and groundwater age at 24 points in Georgia Branch. Groundwater samples of very young apparent age (0-5 years), and stream water from GB387, are plotted at zero age 42

Figure 14. The relationship between PEPA concentration and groundwater age at 24 points in Georgia Branch. Groundwater samples of very young apparent age (0-5 years), and stream water from GB387, are plotted at zero age 42

Figure 15. The relationship between Nafion Byproduct 4 concentration and groundwater age at 24 points in Georgia Branch. Groundwater samples of very young apparent age (0-5 years), and stream water from GB387, are plotted at zero age ... 43

Figure 16. The relationship between PFMOAA concentration and groundwater age at 24 points in Georgia Branch. Groundwater samples of very young apparent age (0-5 years), and stream water from GB387, are plotted at zero age 43

Figure 17. The relationship between PFO3OA concentration and groundwater age at 24 points in Georgia Branch. Groundwater samples of very young apparent age (0-5 years), and stream water from GB387, are plotted at zero age..... 44

Figure 18. The relationship between Nafion Byproduct 2 concentration and groundwater age at 24 points in Georgia Branch. Groundwater samples of very young apparent age (0-5 years), and stream water from GB387, are plotted at zero age ... 44

Figure 19. The relationship between groundwater age and PFAS concentration. Groundwater samples of very young apparent age (0-5 years) are plotted at zero age. Figure from D. P. Genereux..... 45

Figure 20. PFAS concentration and groundwater age, with extrapolations back in time for total PFAS, PMPA, GenX, and PEPA, based on linear trends for each defined by the two oldest age-dated groundwater samples (18 and 28 years old). Extrapolating back to zero concentration provides a crude estimate of the year of earliest groundwater contamination. Only the estimate for GenX is not possible (it predates the start of operations at the plant in 1971); the estimates for total PFAS, PMPA, and PEPA fall between 1979 and 1985, which may be plausible considering the 1971 start date for the plant (1980 is the earliest year for which Chemours acknowledges that GenX was released to air at the manufacturing plant). In principle, the year of earliest groundwater contamination should post-date the first year of PFAS emission to air by a lag time associated with the PFAS transport time through the unsaturated zone. Figure by D. P. Genereux..... 46

Figure 21. The transit time distribution of total PFAS discharging from groundwater at 24 points in the Georgia Branch stream. All PFAS discharge associated with groundwater of very young apparent age (0-5 years) is accounted for in the point plotted at zero age..... 48

Figure 22. The transit time distribution of GenX discharging from groundwater at 24 points in the Georgia Branch stream. All GenX discharge associated with groundwater of very young apparent age (0-5 years) is accounted for in the point plotted at zero age..... 48

Figure 23. Interbedding of sand and clay layers along the western bank of Georgia Branch about 30 m downstream of the zero point 52

1. Introduction

Thousands of per- and polyfluoroalkyl substances (PFAS) have been manufactured since the 1940s. PFAS are manmade chemicals that consist of partially and fully fluorinated carbon chains (Wang et al., 2017). They are highly persistent, bioaccumulative, and toxic (Wang et al., 2017). Of particular interest in North Carolina is GenX, an emerging short-chain PFAS produced as a byproduct at the Chemours Company in Bladen County, North Carolina since 1980 (Hopkins et al., 2018).

In June 2017, the Chemours Company was ordered by the North Carolina state government to cease the release of all process wastewater into the Cape Fear River; however, PFAS are still being detected at high levels in the region, particularly in groundwater discharging from the surficial aquifer to surface water (Koropeckyj-Cox, 2019). Some residents of the area around the Chemours Company have been warned not to consume water from their wells due to the PFAS contamination, and PFAS have been found in the Cape Fear River as far downstream as Wilmington, North Carolina, about 130 kilometers southeast of the chemical plant (Sun et al., 2016).

The coupled discharge of groundwater and PFAS to streams has previously been studied at Georgia Branch and other streams that are tributaries to the Cape Fear River near the Chemours Company (Koropeckyj-Cox, 2019). However, the age of groundwater discharging in the region is unknown. Having information on groundwater flux, PFAS flux, and groundwater age provides new insights about how long PFAS has been entering the surficial aquifer around the Chemours Company and how long it might take for PFAS to be flushed from the aquifer by groundwater flow in future years.

Groundwater transit time is a parameter relevant to the flushing of contaminants from an aquifer into streams and other surface water systems. Groundwater transit time is the time it takes for water to move through an aquifer from recharge at the water table to discharge at a streambed (Lindsey et al., 2003). Transit time is the age of the groundwater just before it leaves an aquifer by discharging into surface water (Gilmore et al., 2016a). An aquifer has a distribution of transit times (not just a single transit time) because some pathways through an aquifer are relatively short and shallow (e.g., for recharge near a stream) while others are longer and deeper (Gilmore et al., 2016a).

Objectives were:

1. Collect and interpret data on groundwater age, water flux (specific discharge), and PFAS concentration and flux at 24 points in the Georgia Branch streambed, following methods developed at NC State in prior work on nitrate contamination (Kennedy et al., 2009a,b; Gilmore et al., 2016a,b).
2. Determine the relationship between PFAS concentration and age of the groundwater discharging into Georgia Branch.
3. Evaluate whether the data could be used to estimate transit time distributions (*TTD*s) of the groundwater and PFAS discharged from the surficial aquifer to the study stream.
4. Evaluate other aspects of the timing and magnitude of groundwater PFAS contamination, as the data allow.

2. Background on PFAS

2.1. Structure and properties of PFAS

Two main subtypes of PFAS have been defined in contemporary literature: legacy and emerging PFAS. Legacy PFAS are fluoroalkyl chains that have been predominantly used and discovered in the environment in the past decades (Sun et al., 2016; Buck et al., 2011). Emerging PFAS are normally shorter fluoroalkyl chains and fluorinated alternatives that are hypothesized to have less of an immunosuppressant effect on humans than legacy PFAS (Sun et al., 2016; Buck et al., 2011). Emerging PFAS are so named because they have been recently replacing legacy PFAS in commercial and industrial applications and are more recently detected in the environment (Sun et al., 2016; Buck et al., 2011).

Major PFAS contamination at the study site was discovered after large amounts of GenX, an emerging PFAS, were documented in the Cape Fear River downstream of the Fayetteville Works (Sun et al., 2016). GenX is a proprietary trade name that refers to an ammonium salt of the hexafluoropropylene oxide dimer acid (HFPO-DA) (Bao et al., 2018). GenX has been used as a replacement for perfluorooctanoic acid (PFOA), a legacy compound, when manufacturing food-contact paper coating and other nonstick coatings (Sun et al., 2016).

2.2. GenX and HFPO-DA

GenX, an ammonium salt, and HFPO-DA, an acid, are two PFAS that have been discussed, often interchangeably, in PFAS literature. When dissolved in water, HFPO-DA loses its proton from the carboxylic acid functional group and GenX loses its ammonium group, and they both form the same carboxylate anion (Hopkins et al., 2018) (Fig. 1). According to the International Union of Pure and Applied Chemistry (IUPAC), the chemical name of GenX is

ammonium 2,3,3,3-tetrafluoro-2-(heptafluoropropoxy)propanoate, and of HFPO-DA is 2,3,3,3-tetrafluoro-2-(heptafluoropropoxy)propanoic acid (Hopkins et al., 2018). HFPO-DA and perfluoro-2-propoxypropanoic acid (PFProPrA) are structurally the same chemical and these names are used interchangeably.

The carboxylate anion of these two molecules in water is referred to as HFPO-DA in recent literature, including a report by Geosyntec commissioned by The Chemours Company (2018), and in Xiao (2017) and Sun et al. (2015). However, in the consent order produced by the NC Department of Environmental Quality (NC DEQ) for the Chemours Company, the common carboxylate anion of GenX and HFPO-DA that is found in surface and groundwater is referred to as GenX (NC DEQ 2019c); this is also true in Hopkins et al. (2018) and Gebbink et al. (2017). Thus, not all authors are using the same name for the carboxylate anion of GenX/HFPO-DA in current literature. I will refer to this aqueous molecule as GenX to remain consistent with papers being published by authors at North Carolina State University (even though, technically, "GenX" refers to the ammonium salt of the HFPO-DA anion).

Table 1. The molecular formulas and structures of GenX and HFPO-DA and their common anion when in water. Molecular images are from the EPA Comptox Database (Comptox, 2019).

Common Name	Molecular Formula	Structure
GenX CAS 62037-80-3	$C_6H_4F_{11}NO_3$	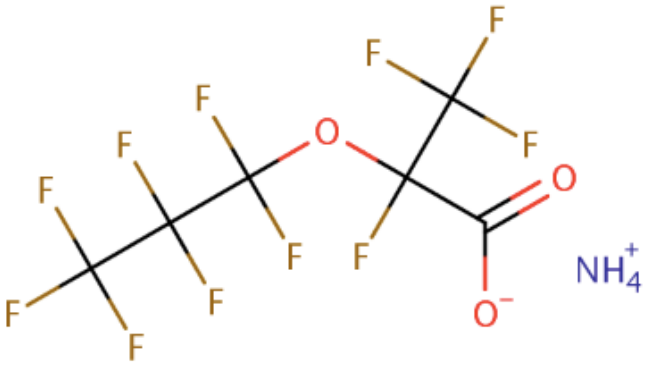
HFPO-DA CAS 13252-13-6	$C_6HF_{11}O_3$	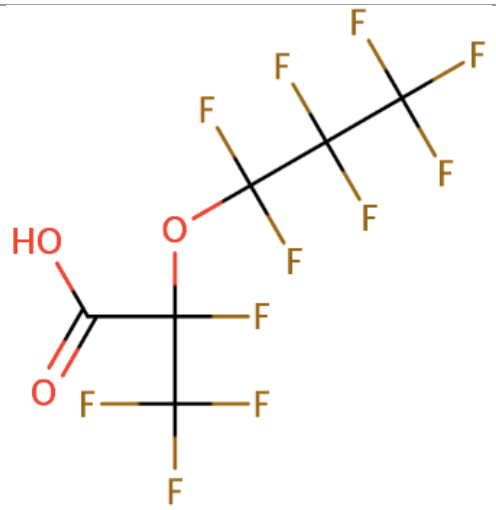
Common Anion	$C_6F_{11}O_3^-$	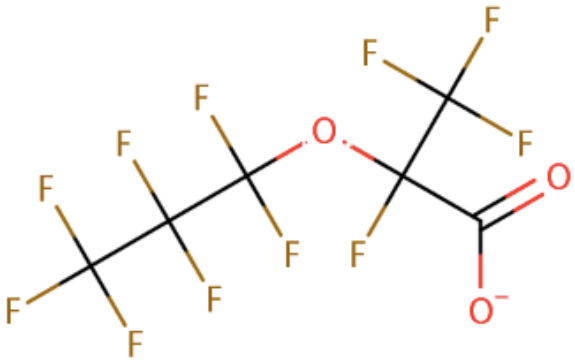

2.3. Background of GenX and other PFAS at the study site

The Fayetteville Works property has been in use since the early 1970s. In 1972, an unlined lagoon was constructed on the property for the handling of biosludge generated from Butacite® (an acetic acid) production. The use of this lagoon was discontinued in 1979. Two other unlined lagoons were in use from 1979 to 1990 (DuPont, 2002). Nafion® has been produced and stored at the Fayetteville Works since, at least, October 1980 when there were 2 Nafion® caustic waste and acids tanks, Nafion caustic water storage tanks, a 100' by 300' Nafion ® drum storage, and 4 Nafion ® waste fluorocarbon and hydrocarbon tanks (E.I. DuPont, 1980). By 1980, GenX was also being produced at the site and treated wastewater was released to the Cape Fear River (Hopkins et al., 2018).

In 2016, the United States Environmental Protection Agency (EPA) set drinking water health advisories for PFOA and PFOS, two legacy PFAS, at 70 ng L^{-1} (US EPA, 2016). As of July 2017, the North Carolina Department of Health and Human Services has issued a drinking water health goal for GenX of 140 ng L^{-1} (NC DEQ, 2017a).

In 2017, the Chemours Company stated that HFPO-DA had been released from an on-site wastewater treatment plant to the Cape Fear River since 1980, as GenX and HFPO-DA were created as by-products without any commercial intent and, therefore, excluded from a capture order requirement mandated by the EPA (Hopkins et al., 2018). As of June 2017, the state of North Carolina has ordered the Chemours Company to cease the release of effluent from the plant to surface water (NCDEQ, 2017a).

A February 26th 2019 consent order signed by the state and the North Carolina Department of Environmental Quality (NC DEQ), the Cape Fear River Watch, and the Chemours Company FC, LLC. stated that the Chemours Company was required to install

abatement technology, including a thermal oxidizer, at its facility to reduce annual air emissions of GenX compounds and other PFAS by at least 99% of baseline levels (NCDEQ, 2019c). This order also called for continued capturing and subsequent offsite disposal of all process wastewater unless new authorization is issued as a National Pollutant Discharge Elimination System permit (NCDEQ, 2019c).

Air quality sampling near the Chemours Company by the NC DEQ's Division of Air Quality began in January 2018 to assess the deposition of GenX from air emissions at the Fayetteville Works (NC DEQ, 2018). From March 20th to the 27th in 2018, rainwater collected 2 to 3 km southwest of the Fayetteville Works showed concentrations of 111 and 104 ppt (NC DEQ, 2018). In the same area, rainwater fluctuated in GenX concentrations between about 100 and 750 ppt from 2018 through February 2019 (NC DEQ, 2018).

The NC DEQ Division of Air Quality has estimated the amount of PFAS emitted to the air from 2012 to 2016. The precursor chemical to PMPA is estimated to have ranged from 12,020 lbs/year in 2012 to 16,467 lbs/year in 2014 to 14,188 lbs/year in 2016. The precursor to GenX was estimated to have been emitted amounts ranging from 2,820 lbs/year in 2016 to 11,167 lbs/year in 2014. The precursors to PEPA, PFO2HxA, PFO3OA, and PFMOAA, listed in decreasing order of concentration, were estimated to have been released at lower concentrations than PMPA and GenX (NCDEQ, 2018). Emission rates in 2019 may have been significantly lower than in the period from 2012 to 2016, as the GenX emission reported by Chemours for 2019 was only 144 pounds (NCDEQ, 2019c).

3. Background on tritium-helium age dating

Tritium-helium age dating relies on the radioactive decay of tritium (^{3}H). Tritium is a radioactive isotope of hydrogen, with a half-life of 12.43 years, which decays to helium-3 (^{3}He) (Schlosser et al., 1988). Natural ^{3}H from the upper atmosphere is incorporated into water molecules and enters the hydrologic cycle (Schlosser et al., 1988). When these tritiated water molecules fall to earth as precipitation and enter groundwater systems as recharge, the groundwater ^{3}H/^{3}He ratio decreases with time and acts as a tracer for the length of time water has been in the saturated zone accumulating tritiogenic ^{3}He (Schlosser et al., 1988; Poreda et al., 1988). The usual form of the age dating equation used is (Solomon et al., 1992):

$$t = \lambda^{-1} \ln\left(1 + \frac{[^3He^*]}{[^3H]}\right) \quad (1)$$

where t is the age of the groundwater, λ is the radioactive decay constant for ^{3}H (0.05576 yr^{-1}), [^{3}H] is the tritium content of the groundwater in tritium units (TU), and [^{3}He*] is the content of tritiogenic ^{3}He in the groundwater (i.e., the ^{3}He produced by ^{3}H decay in the groundwater), also expressed in TU (e.g., Schlosser et al., 1989).

In addition to measuring ^{3}He, other noble gases (^{4}He, Ne, Ar, Kr, Xe) are often analyzed to estimate the groundwater recharge temperature (Heaton and Vogel, 1981) and for the estimation of [^{3}He*], a portion of the total dissolved ^{3}He in the sample (Solomon et al., 1992, Gilmore et al., 2016a). To determine whether the ^{3}H/^{3}He ratio in groundwater has been affected by degassing or by the dissolution of "excess air," these noble gases must be measured (Heaton and Vogel, 1981). Degassing and excess air will influence the interpretation of ^{3}H/^{3}He age estimates (Poreda et al., 1988; Gilmore et al., 2016a).

4. Study area

4.1. Coastal Plain hydrogeology

The study site is the Georgia Branch watershed, a 21.9 km^2 tributary watershed to the Cape Fear River. The sampling sites within the Georgia Branch watershed were about 3 km south of the Fayetteville Works property. The Georgia Branch watershed is located in the Cape Fear River basin which contains the cities of Greensboro, Fayetteville, Elizabethtown, and Wilmington. The latter two cities are located along the Cape Fear River and downstream of the Chemours Company. Georgia Branch is normally a gaining stream, receiving groundwater input from its surrounding watershed (Fig. 1) (Koropeckyj-Cox, 2019).

4.2. Local geology

The Georgia Branch watershed is in the Sand Hills, the westernmost part of the N.C. Coastal Plain. In this region, the surficial geologic layer consists of unconsolidated, permeable sand with clay lenses (Winner et al., 1989). The surficial aquifer gradually thickens eastward from the Sand Hills to the Atlantic coast (Giese et al., 1997). Below the surficial aquifer are, from top to bottom, the Black Creek confining unit, the Black Creek aquifer, the Upper Cape Fear confining unit, and the Upper Cape Fear aquifer (Fig. 3) (Giese et al., 1997; NCDEQ, 2019a). These layers overlay crystalline basement rock (Giese et al., 1997).

The Coastal Plain geology is formed by a series of down-stepping paleo-coastlines and nested, embayed paleo-valleys that are not unconformity-bounded units (Abbott et al., 2011). Along the Cape Fear River are four Cretaceous formations made of mostly siliclastic materials (Abbott et al., 2011). The facies of each of these formations are interpreted as ancient fluvial

channels and floodplains (Abbott et al., 2011). These paleo-channels consist of sands, clays, and gravels which include quartz, rock fragments, and petrified wood (Abbott et al., 2011).

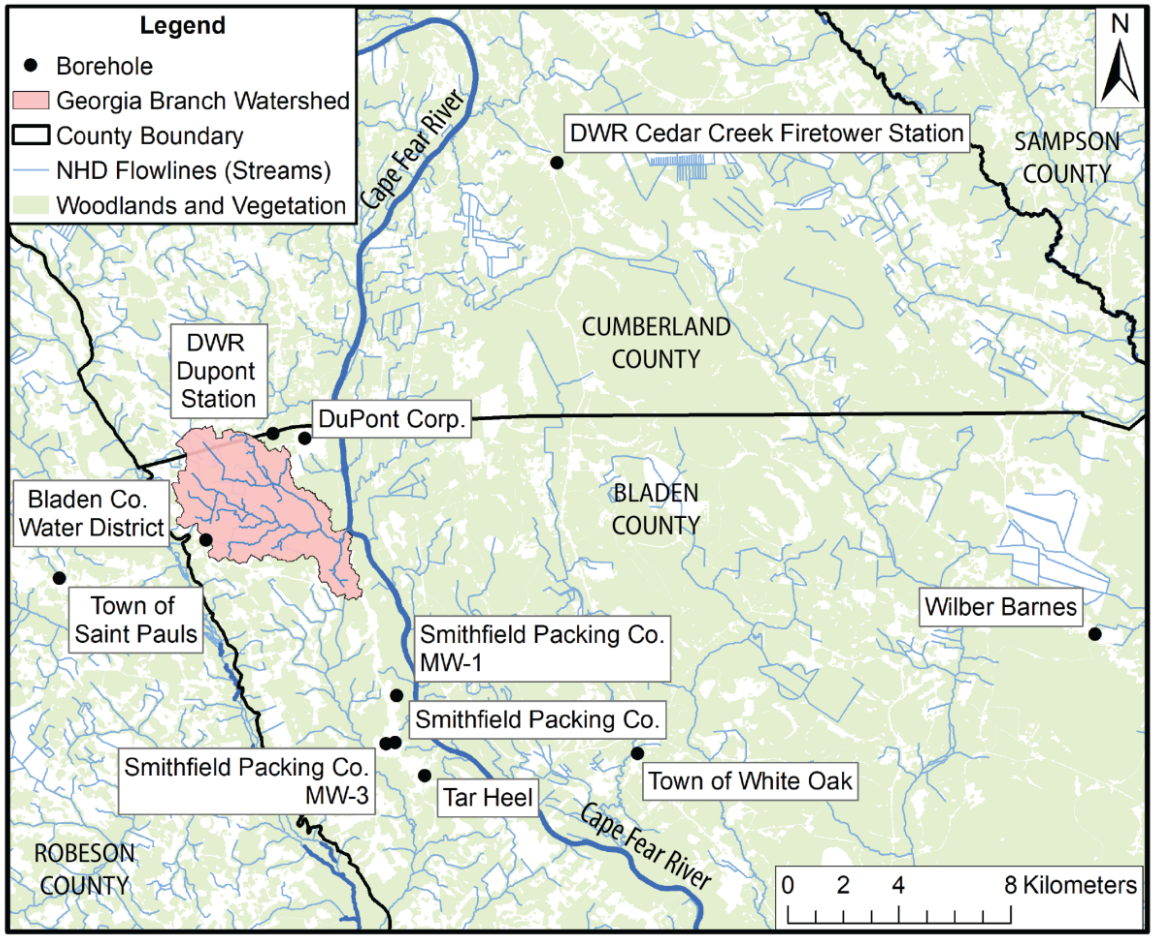

Figure 1. 11 NCDEQ boreholes where borehole stratigraphy has been measured (NCDEQ 2019a). NHD refers to the USGS's National Hydrography Dataset. The name of each borehole is shown in a white box on the map. The base map was created using shapefiles provided by the USGS (USGS Map, 2016a-l).

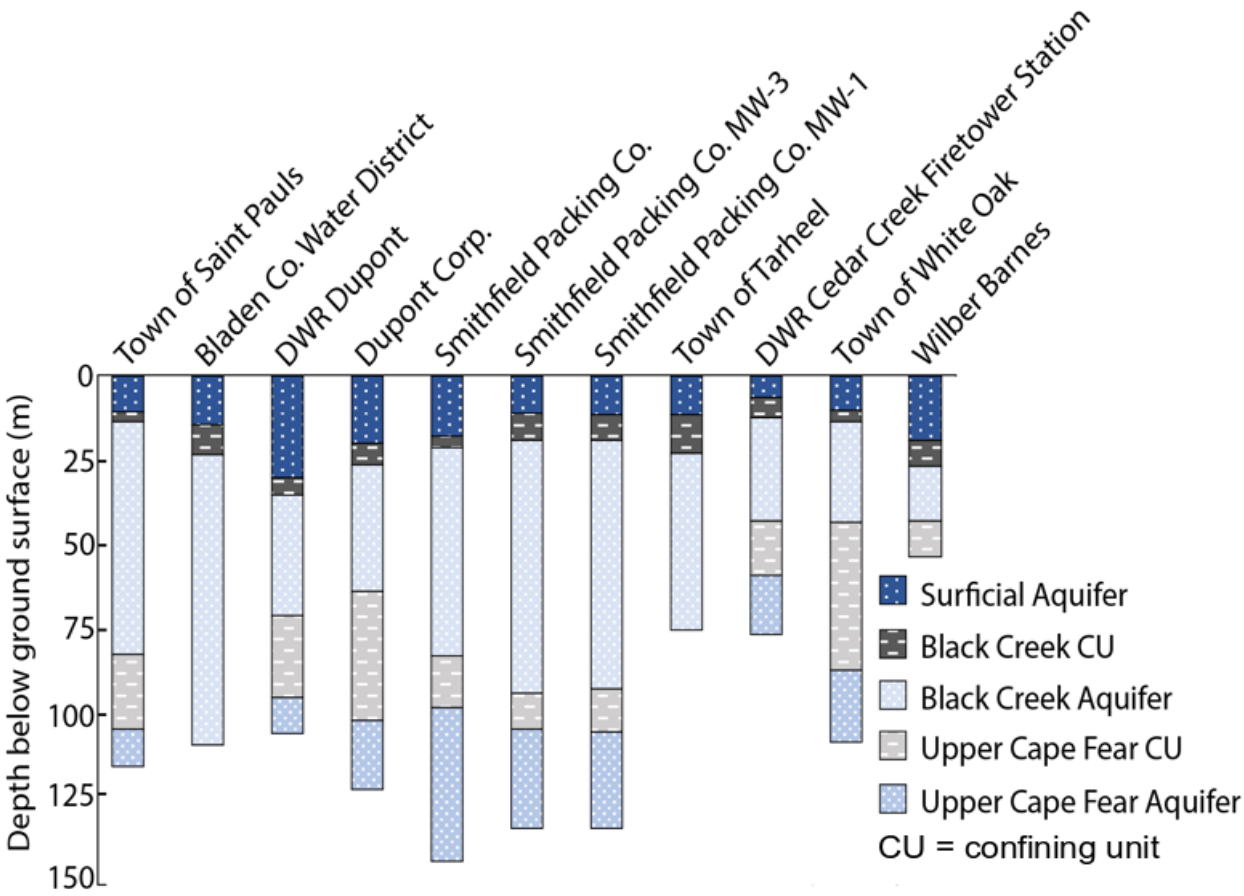

Figure 2. Hydrostratigraphy of the 11 boreholes shown in Fig. 2, ordered from west, on the left, to east, on the right (NCDEQ, 2019a). The bottom of each column represents the bottom of the borehole, not necessarily the bottom of the deepest layer shown. The average stratigraphic thickness of the surficial aquifer in this area is 15.9 m.

The elevation of the ground surface at the study site in Georgia Branch, near the DuPont Corp. well, ranges from 20 to 30 m above sea level. The total stratigraphic thickness of the surficial aquifer at the DuPont Corp. well is 19.2 m (Fig. 2), and a 10.5 m deep well is used to monitor the water table elevation at the DuPont Corp. borehole located on the Fayetteville Works property. This well and borehole are the closest pairing to the study site available (Fig. 1). At this well, the surficial aquifer had an average saturated thickness (water table to the bottom of the aquifer) of 14 m from January 2004 to January 2019 (Fig. 3). The average saturated thickness was calculated by subtracting the depth of the water table at the DuPont Corp. well from the total

stratigraphic thickness of the surficial aquifer (ground surface to the bottom of the aquifer) at the same well.

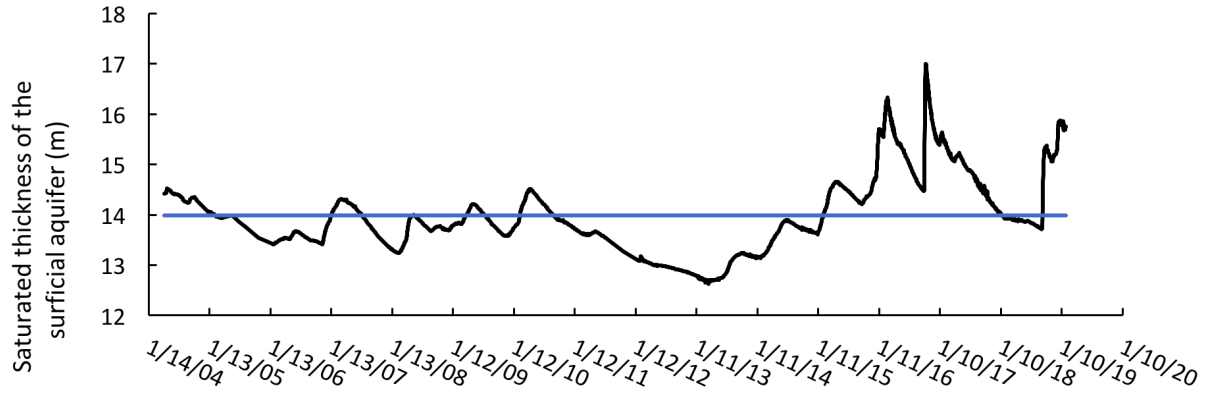

Figure 3. The saturated thickness of the surficial aquifer at the DuPont Corporation well, located at the Chemours Company (Figs. 1, 2), as monitored by the NC Department of Environmental Quality's Division of Water Quality from April 4, 2004 to February 3, 2019 (NCDEQ, 2019b). Mean saturated thickness from 2004 to 2019, 14 m, is indicated by the blue line.

4.3. Climate

Fayetteville, North Carolina has an annual average daily high temperature of 22.5°C and the average daily low temperature is 9.9°C; the annual average temperature is 16.2°C (US Climate Data, 2019). The average annual precipitation from rainfall is 115 cm, and snow accumulation is rare (US Climate Data, 2019). The highest amount of precipitation occurs over the summer months, peaking in August with an average precipitation of 14 cm (US Climate Data, 2019). Like the surrounding southeast US, the Cape Fear River basin has a humid subtropical climate (NC Climate, 2012).

4.4. Land and water use

Excluding the urban area around Fayetteville in northwestern Cumberland County, the majority of land use in Cumberland and Bladen Counties consists of forested wetlands and agricultural fields. These agricultural fields produce tobacco and cotton, primarily. According to

the USGS, the 2015 population of Bladen County was 34,318. Of the total population, less than half were served by public supply sourced from groundwater. More than 18,000 people received water from domestic wells (USGS Water Data, 2015).

5. Study Design

This research consisted of one phase of data collection. The reach of Georgia Branch used for sampling here was previously used by Koropeckyj-Cox (2019) for measuring coupled groundwater and PFAS fluxes. Georgia Branch is an ideal location for groundwater sampling due to the sandy streambed and because it is a gaining stream. The studied reach is accessible with sampling equipment and mostly clear of vegetation that may obstruct sampling methods.

A sampling campaign was carried out over the 25th and 26th of February 2019. Groundwater flux and groundwater-based PFAS flux through the streambed of Georgia Branch were found at 24 points in a 530 m reach of Georgia Branch (Fig. 5). Groundwater samples needed for tritium-helium age dating were also collected from within 10 cm of each flux measurement point.

Groundwater samples were collected from 35 cm below the streambed of Georgia Branch over a 2-day campaign. Vertical hydraulic head gradients and hydraulic conductivity measured in Georgia Branch were used to calculate groundwater flux. Separate groundwater samples were collected for the analysis of the concentrations of PFAS, tritium-helium, and noble gases. The 24 sampling points were alternated between the left, center, and right of the stream channel. At 5 sections of the stream channel (330 m, 387 m, 412 m, 450 m, and 490 m downstream of the "zero" point at 34.815820°, -78.831911°), three-point transects were taken perpendicular to the stream, so that left, center, and right measurements and samples were taken.

6. Methods

6.1. Specific discharge

Water flux (specific discharge, v) was calculated at each of the 24 sampling points in the Georgia Branch streambed as $v = KJ$, where K and J are the hydraulic conductivity and vertical hydraulic head gradient, respectively, at a point. K was found using a falling head test with a field permeameter that was inserted 35 cm into the streambed (Genereux et al., 2008). At each measurement point, the falling head test was performed after the vertical hydraulic head gradient was measured, and after groundwater samples were obtained for PFAS, tritium, and noble gas analysis. The calculation of K was based on the Hvorslev (1951) method as used by Genereux et al. (2008). Ambient head inside the permeameter, before the falling head test, was estimated as the height of the surface water on the outside of the permeameter plus the product of the vertical head gradient in the streambed and the depth of penetration of the permeameter in the streambed (35 cm) (Genereux et al., 2008).

At each point in Georgia Branch, the vertical hydraulic head gradients were interpreted using a light oil-water manometer attached to a steel piezometer inserted 35 cm into the streambed (Kennedy et al., 2007). 35 cm is likely below the hyporheic zone where groundwater and surface water mix. The steel piezomanometer was left to equilibrate for 15 to 20 minutes at each sampling location after purging 250-300 mL of groundwater. When equilibrated, groundwater and surface water head values and air and streambed temperatures were recorded. To obtain the actual head difference between groundwater and stream water, the measured head difference from the piezomanometer was divided by the amplification factor based on the temperature-density relationships of the oil and water in the manometer (Kennedy et al., 2007).

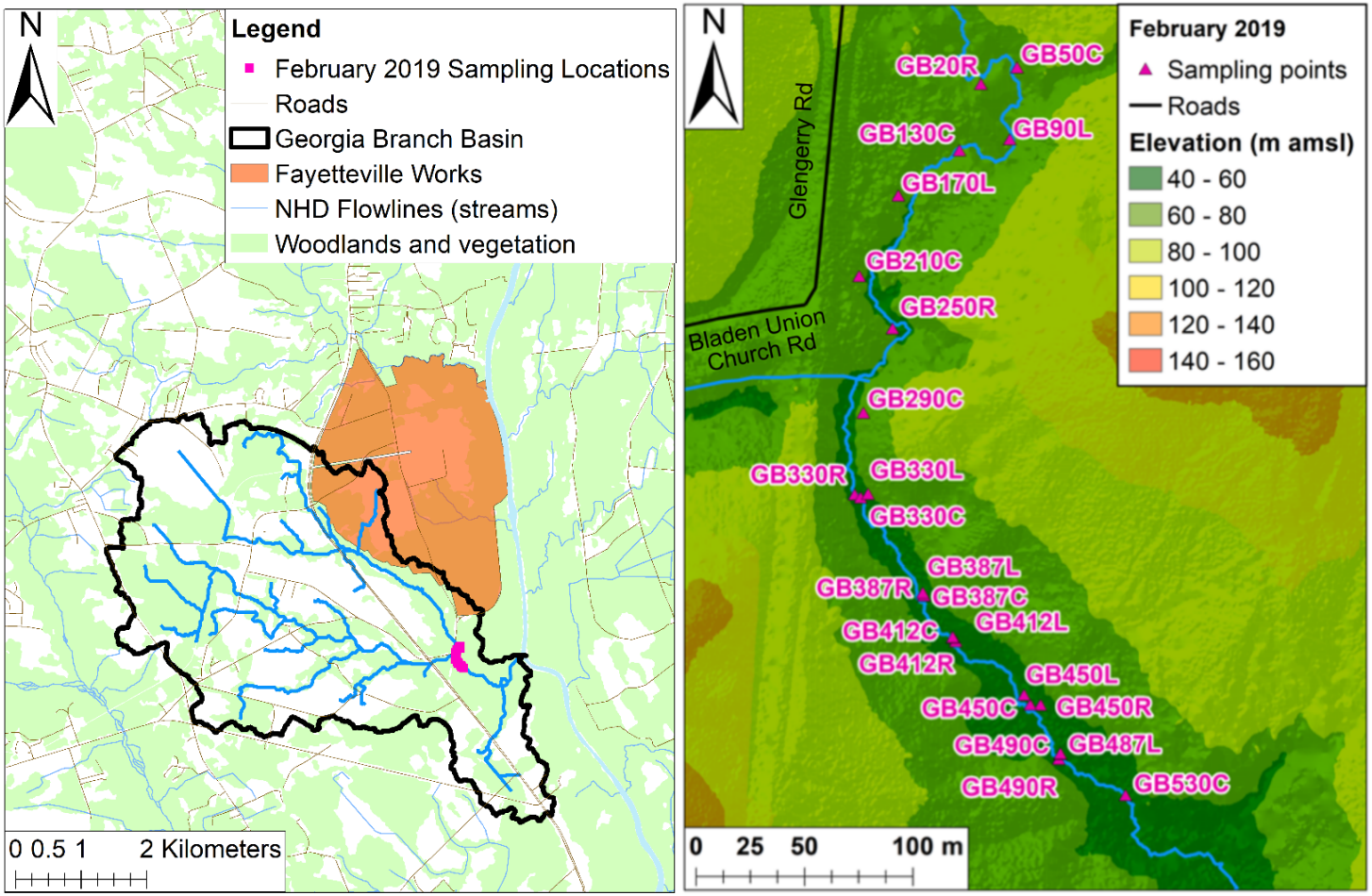

Figure 4. Left image shows the locations of the Fayetteville Works and the Georgia Branch watershed. On the right, the Georgia Branch streambed sampling points are labeled on a Digital Elevation Model (DEM).
Data for the delineation of the Georgia Branch watershed comes from the 1-meter DEMs provided by the USGS, NHD refers to the USGS's National Hydrography Dataset. (USGS Map, 2017). The left base map is modified from the USGS Topo Map Data and Topo Style Sheet, downloaded from The National Map (USGS Map, 2016a,b). The close up of Georgia Branch was defined by Blake Baines from NCSU using LiDAR data provided by North Carolina's Spatial Data Download and displayed by M.A. Pétré on a DEM from the USGS (USGS Map, 2017; USGS, 2016d).

6.2. PFAS flux and concentration

At each streambed measurement point, PFAS flux through the streambed (f_{PFAS}) was calculated as $f_{PFAS} = v$[PFAS], where v is the specific discharge through the streambed at the point and [PFAS] is the concentration of PFAS (either an individual chemical or the sum of all measured PFAS) in the groundwater beneath the streambed at that point. PFAS fluxes were calculated as mg of PFAS per m^2 of streambed per day.

Groundwater samples for PFAS analysis were drawn up from the streambed through the stainless-steel screen and copper sampling line of a piezometer using a polypropylene syringe with a 3-way stopcock that was connected to the piezometer with about 40 cm of clear flexible PVC tubing. The water was discharged from the syringe through the stopcock into 50 mL Clarified Polypropylene Falcon conical centrifuge tubes. Each centrifuge tube was rinsed three times with about 20 mL of groundwater. PFAS concentrations were analyzed in the laboratory of Dr. Detlef Knappe in the Department of Civil, Construction, and Environmental Engineering at NCSU using a liquid chromatography-mass spectrometry (LCMS) system to quantify 27 different PFAS in groundwater samples (Table 2). The minimum reporting level for all PFAS compounds was 5 ng L^{-1}.

Table 2. The PFAS compounds for which the groundwater samples were analyzed, their acronyms, and molecular formulas.

Common Acronym	CAS Number	Name	Molecular Formula
PFBA	375-22-4	perfluorobutanoic acid	$C_3F_7CO_2H$
PFPeA	2706-90-3	perfluoropentanoic acid	$C_5HF_9O_2$
PFHxA	307-24-4	perfluorohexanoic acid	$C_6HF_{11}O_2$
PFHpA	375-85-9	perfluoroheptanoic acid	$C_7HF_{13}O_2$
PFOA	335-67-1	perfluorooctanoic acid	$C_8HF_{15}O_2$

Table 2 (continued).

PFNA	375-95-1	perfluorononanoic acid	$C_9HF_{17}O_2$
PFDA	335-76-2	perfluorodecanoic acid	$C_{10}HF_{19}O_2$
PFBS	375-73-5	perfluorobutanesulfonic acid	C_4HF_9O3S
PFPeS	2706-91-4	perfluoropentanesulfonic acid	$C_5HF_{11}O_3S$
PFHxS	108427-53-8	perfluorohexanesulfonate	$C_6F_{13}O_3S$
PFHpS	375-92-8	perfluoroheptanesulfonic acid	$C_7HF_{15}O_3S$
PFOS	1762-23-1	perfluorooctanesulfonic acid	$C_8HF_{17}O_3S$
4:2 FTS	757124-72-4	4:2 fluorotelomer sulfonic acid	$C_6H_5F_9O_3S$
6:2 FTS	27619-97-2	6:2 fluorotelomer sulfonic acid	$C_8H_5F_{13}O_3S$
NVHOS	801209-99-4	1,1,2,2-tetrafluoro-2-(1,2,2,2-tetrafluoroethoxy)ethane sulfonic acid	$C_4H_2F_8O_4S$
Nafion Bp 1	29311-67-9	2-[1-[difluoro[(1,2,2-trifluoroethenyl)oxy]methyl]- 1,2,2,2-tetrafluoroethoxy]-1, 1,2,2-tetrafluoro-ethanesulfonic acid	$C_7HF_{13}O_5S$
Nafion Bp 2	749836-20-2	2-[1-[difluoro(1,2,2,2-tetrafluoroethoxy)methyl]- 1,2,2,2-tetrafluoroethoxy]- 1,1,2,2-tetrafluoro-ethanesulfonic acid	$C_7H_2F_{14}O_5S$
Nafion Bp 4	N/A	2,2,3,3,4,5,5,5-4-(1,1,2,2-tetrafluoro-2-sulfoethoxy)pentanoic acid	$C_7H_2F_{12}O_6S$
PFO4DA	39492-90-5	perfluoro-3,5,7,9-tetraoxadecanoic acid	$C_6HF_{11}O_6$
PFO5DOA	39492-91-6	perfluoro-3,5,7,9,11-pentaoxadodecanoic acid	$C_7HF_{13}O_7$
HydroEve	773804-62-9	2,2,3,3-Tetrafluoro-3-((1,1,1,2,3,3-hexafluoro-3-(1,2,2,2-tetrafluoroethoxy)propan-2-yl)oxy)propanoic acid	$C_8H_2F_{14}O_4$
PFMOAA	674-13-5	difluoro(perfluoromethoxy)acetic acid	$C_3HF_5O_3$
PMPA	13140-29-9	perfluoromethoxypropyl carboxylic acid	$C_4HF_7O_3$
PEPA	267239-61-2	perfluoropentadecanoate	$C_5HF_9O_3$
GenX (HFPO-DA)	13252-13-6	perfluoro-2-propoxypropanoic acid	$C_6HF_{11}O_3$
PFO2HxA	39492-88-1	perfluoro-3,5-dioxahexanoic acid	$C_4HF_7O_4$
PFO3OA	39492-89-2	perfluoro-3,5,7-trioxaoctanoic acid	$C_5HF_9O_5$

6.3. Groundwater age dating

Groundwater samples for tritium were collected in 500 mL low-density and high-density polyethylene bottles (LDPE, HDPE) using the same method described above for the collection of PFAS samples. The bottles were rinsed with 60 mL of groundwater before sampling. Groundwater for noble gas analysis was collected in copper tubes using PVC piezometers, as in Aeschbach-Hertig and Solomon (2013), using an "inertial pumping" method with the copper tube raised and lowered in a quick reciprocating motion inside the piezometer. At one end of the copper tube (the lower end inside the piezometer) was a Waterra Micro Flow Inertial Pump steel check value, at the other end was 3 meters of HDPE tubing connected to a 1/4" HB Series 326 3-Way PVC Ball Valve with Buna-N Seals from US Plastics. Connecting to the opposite hose barb on the valve was a PVC tube for discharge, and connecting to the middle hose barb of the valve was PVC tubing attached to a 60 mL syringe to provide backpressure. Groundwater was pumped through the system until 3-6 times the volume of the copper tube passed and no bubbles remained. Backpressure was then applied as the copper tube was removed from the piezometer and clamped at both ends.

7. Results

7.1. Water flux

In Georgia Branch, during the February 2019 campaign, the arithmetic mean water flux, v, was 1.53 m d^{-1} (Table 3). The standard deviation of v was 1.19 m d^{-1}. Water flux is calculated by multiplying J and K, the arithmetic means of each were 0.0243 and 69.6 m d^{-1}. The geometric mean K was 42.5 m d^{-1}.

In Georgia Branch, during the October 2018 campaign, the arithmetic mean v was 1.45 m d^{-1} (Koropeckyj-Cox, 2019), very close to the mean value in February 2019 (Table 3). Mean v through the streambed at Georgia Branch was larger than in some other NC Coastal Plain streams. For example, in February 2006, at West Bear Creek, mean v was 0.47 m d^{-1} (Kennedy et al., 2009b). In July 2012 and March 2013, average v at West Bear Creek was 0.35 m d^{-1} and 0.40 m d^{-1}, respectively (Gilmore et al., 2016c). At Hominy Swamp Creek, mean v was 0.56 m d^{-1} (Nickels, 2016).

Hydraulic conductivity, K, was much larger at Georgia Branch than in the other Coastal Plain streambeds (Table 3). The relationship between K and v in Georgia Branch gives a coefficient of determination (r^2) of 68.7% (p-value = 3.12 x 10^{-7}) (Fig. 5).

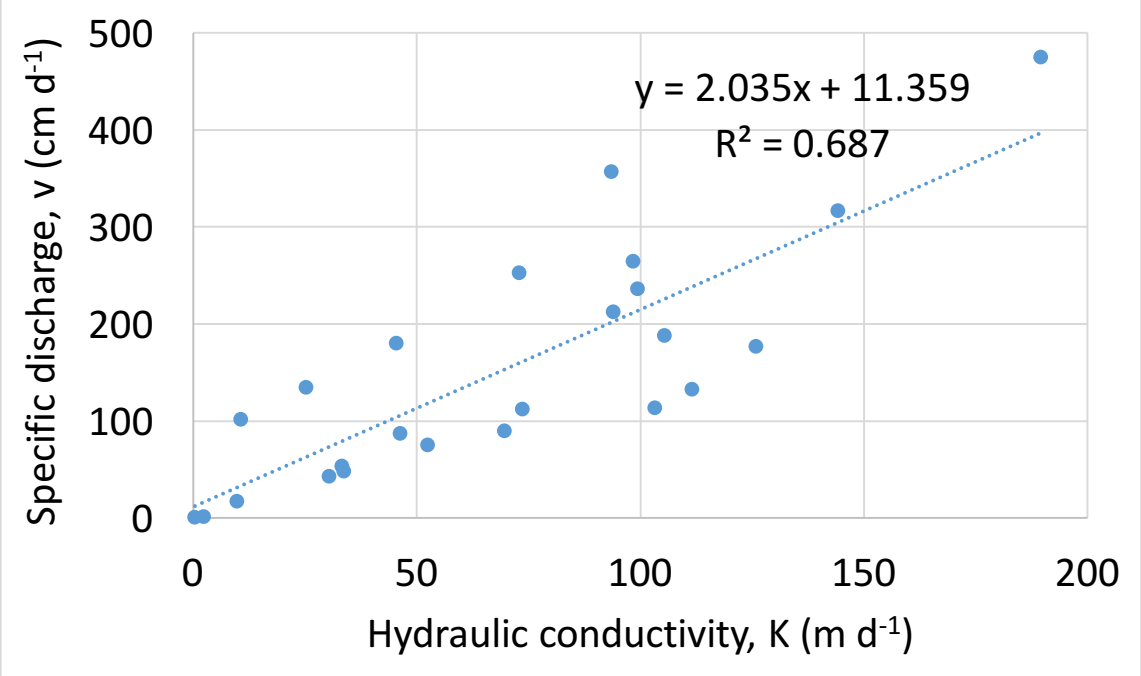

Figure 5. The relationship between hydraulic conductivity, K, and specific discharge, v, in the streambed of Georgia Branch in February 2019.

The standard deviation of ln$K$ may be so different between Georgia Branch measurements in October 2018 and February 2019 due to the location of point measurements in

the streambed. The February campaign alternated between left, center, and right streambed sampling locations. The October campaign was focused on center streambed points and may, therefore, have less variation across *K*. Average *K* was higher in Georgia Branch during the October 2018 sampling campaign, which follows the observations of Genereux et al. (2008) where significantly higher hydraulic conductivity was found in the middle of the stream than along the left and right sides.

Table 3. Comparison of results on streambed *v*, *K*, and *J* between the present study and 4 other studies of streambeds in the North Carolina Coastal Plain.

	Present study: Georgia Branch, February 2019	Georgia Branch, October 2018, (Koropeckyj-Cox, 2019)	Hominy Swamp Creek, January 2016 (Nickels, 2016)	West Bear Creek, February 2006 (Kennedy et al., 2009b)	West Bear Creek, March 2013 (Gilmore et al., 2016c)
v **(m d^{-1}), mean**	1.53	1.45	0.56	0.47	0.40
Standard deviation of *v* (m d^{-1})	1.19	1.38	0.91	0.58	0.85
K **(m d^{-1}), mean**	69.6	100	27.6	15.9	12.9
K **(m d^{-1}), geometric mean**	42.5	89.1	---	---	---
Standard deviation of ln*K*	1.42	0.516	---	---	---
J**, mean**	0.0243	0.0129	0.021	0.036	0.05
Number of points (*n*)	24	21	25	46	30

Table 4. Vertical water flux (*v*), hydraulic conductivity (*K*), and vertical hydraulic head gradient (*J*) for each streambed measurement point in Georgia Branch, 25-26 February 2019. Each point is named by its distance downstream along the channel in meters from the zero point established just east of Glengerry Road in October 2018, and whether it was on the left side, center, or right side of the streambed (L, C, or R, respectively), from the perspective of an observer facing downstream.

Sampling point	*v* (m d^{-1})	*K* (m d^{-1})	*J*
GB20R	1.02	10.6	0.0954
GB50C	2.36	99.4	0.0238
GB90L	0.007	0.380	0.0174
GB130C	1.80	45.5	0.0396
GB170L	0.02	2.37	0.0064
GB210C	1.33	112	0.0119
GB250R	1.12	73.6	0.0152
GB290C	1.14	103	0.0110
GB330L	0.897	69.5	0.0129
GB330C	2.13	93.9	0.0226
GB330R	1.77	126	0.0141
GB387L	0.874	46.3	0.0189
GB387C	0.537	33.3	0.0161
GB387R	0.433	30.4	0.0142
GB412L	2.65	98.3	0.0269
GB412C	3.17	144.2	0.0220
GB412R	3.57	93.4	0.0382
GB450L	0.482	33.7	0.0143
GB450C	1.88	105	0.0179
GB450R	0.756	52.5	0.0144
GB490L	1.35	25.3	0.0534
GB490C	2.53	72.9	0.0347
GB490R	0.171	9.78	0.0174
GB530C	4.75	190	0.0251

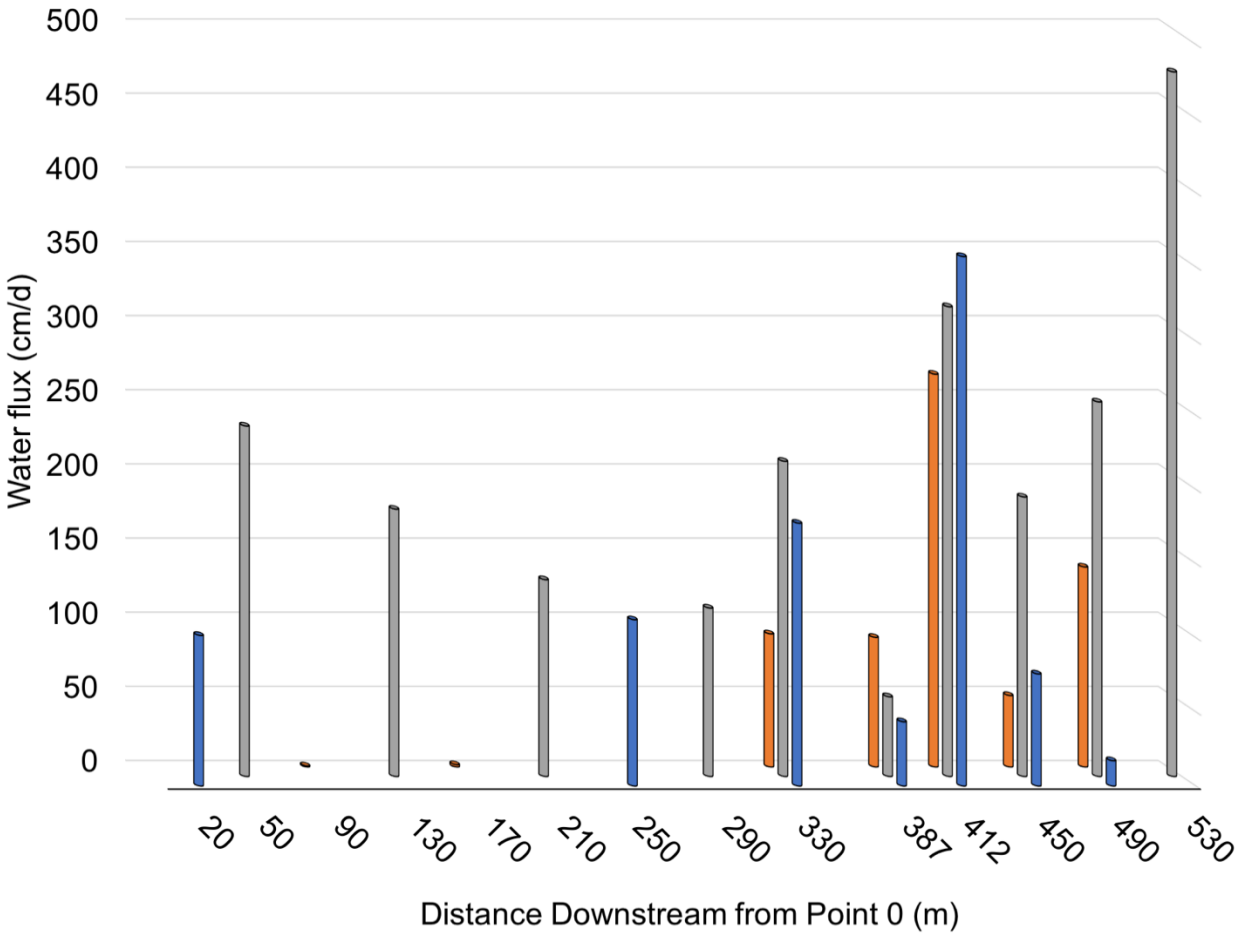

Figure 6. Water flux (specific discharge, *v*) through the streambed of Georgia Branch, 25-26 February 2019. Blue, gray, and orange bars show streambed sampling points on the right side, center, and left side of the channel, respectively. Three point transects across the channel were sampled at 330 m, 387 m, 412 m, 450 m, and 490 m. A point on the left side of the channel was not feasible at the 490 m transect, but measurements were made at 487L, and the water flux at 487L is plotted above as part of the 490 m transect.

7.2. PFAS concentrations and flux

Of the 27 PFAS compounds measured, 13 compounds were below the minimum reporting level (MRL) of 5 ng L^{-1} at all 24 sampling points: PFHxA, PFOA, PFNA, PFDA, PFBS, PFHxS, PFHpS, PFOS, 4:2 FTS, 6:2 FTS, NVHOS, Nafion Bp 1, and PFO5DoA. The eight most abundant PFAS compounds, which make up 99.78% of the total measured PFAS concentration in the 24 groundwater samples, are PMPA (37.9%), GenX (23.4%), PFO2HxA

(16.7%), PEPA (13.6%), Nafion Bp 4 (3.10%), PFMOAA (2.56%), PFO3OA (2.02%), and Nafion Bp 2 (0.482%) (Table 3, Fig. 8). Three PFAS were present at relatively low levels: PFBA (0.105%), PFPeA (0.0690%), and PFO4DA (0.0511%) (Table 5, Fig. 7).

The mean total PFAS concentration in groundwater was 2039 ng L^{-1} for all 24 measurement points. In Georgia Branch during October 2018 (Koropeckyj-Cox, 2019), the mean total PFAS concentration of groundwater was 2306 ng L^{-1} (n=22). The smallest total PFAS concentration of the sampling points was 313 ng L^{-1} at GB412R, and the highest total concentration was found at GB290C at 4773 ng L^{-1}. Most of the groundwater GenX concentrations were well above the health goal of 140 ng L^{-1} for GenX in drinking water (NC DEQ 2017). The average GenX concentration of the 24 points was 477 ng L^{-1}, and only four sampling points had GenX concentrations below the health goal: GB250R (124 ng L^{-1}), GB412R (91 ng L^{-1}), GB490L (73 ng L^{-1}), and GB490C (114 ng L^{-1}).

Compared with a stream water sample taken at GB387, stream water had lower than detectable concentrations of PFMOAA and groundwater had an average concentration of 52 ng L^{-1} of PFMOAA. Seven groundwater samples contained concentrations of PFMOAA below minimum reporting levels. The stream water concentrations of PMPA, PEPA, GenX, PFO2HxA, PFO3OA, and Nafion Byproduct 2 were higher than the average groundwater values for each compound. The higher concentrations of certain PFAS in stream water may indicate that these compounds are discharged at higher concentrations upstream of the groundwater sampling sites.

In February 2019, the mean PFAS flux from groundwater into Georgia Branch was 2.90 mg m^{-2} d^{-1} and the mean GenX flux was 0.718 mg m^{-2} d^{-1} (Table 6, Fig. 8). Similar flux was observed in October 2018, when the mean PFAS flux into Georgia Branch was 3.01 mg m^{-2} d^{-1}, and the mean flux of GenX was 0.75 mg m^{-2} d^{-1} (Koropeckyj-Cox, 2019).

PFAS flux is necessary to understand the movement of PFAS through the watershed, and, in principle, spatial variability of this flux is controlled by spatial variability in both PFAS concentrations and groundwater flux. The concentration data indicate the mass of PFAS per volume of water resident in different areas of the groundwater discharge zone, while flux indicates the actual discharge rate of PFAS into the stream through groundwater discharge.

The coefficient of variation (CV) of total PFAS flux (1.08) is lower than that of total PFAS concentration (2.04), and closer to that of groundwater flux (1.29) (Table 7). This similarity may suggest that spatial variability in groundwater flux is an important control of spatial variability in the flux of PFAS discharging from the groundwater to Georgia Branch stream water. The variability in water flux is determined largely by the variation in hydraulic conductivity, *K*, in Georgia Branch ($r^2 = 68.7\%$); therefore, the spatial variability in PFAS flux discharging from the groundwater to Georgia Branch (Fig. 8) seems to be highly dependent on the spatial variability of *K* in the streambed. This dependence suggests the scale and pattern of variability of PFAS flux in Georgia Branch and, perhaps, other streams may be mostly controlled by this physical hydrogeological variable, streambed *K*.

Koropeckyj-Cox (2019) estimated the area of the Georgia Branch streambed to be 11800 m^2 and the total area of the Mines Creek streambed, a large tributary to the Georgia Branch stream located 280 m downstream of the zero point, as 11600 m^2 (both areas include all minor tributaries shown in Fig. 4). Using these streambed area estimates, total PFAS discharge from groundwater to Georgia Branch was estimated by multiplying mean PFAS flux by the total streambed area. For Georgia Branch alone, this calculation suggests that 34.3 g of PFAS per day and 8.47 g of GenX per day were discharged from groundwater into the stream on the dates of sampling in February 2019. For Georgia Branch and Mines Creek together (i.e., the full channel

network in the Georgia Branch watershed), a total of 67.9 g of PFAS per day and 16.8 g of GenX per day are estimated to have discharged from groundwater to the streams on the dates of sampling. The corresponding estimate for October 2018 was 59.6 g of total PFAS per day discharged from groundwater into Mines Creek and Georgia Branch (Koropeckyj-Cox, 2019), very close to the February 2019 estimate.

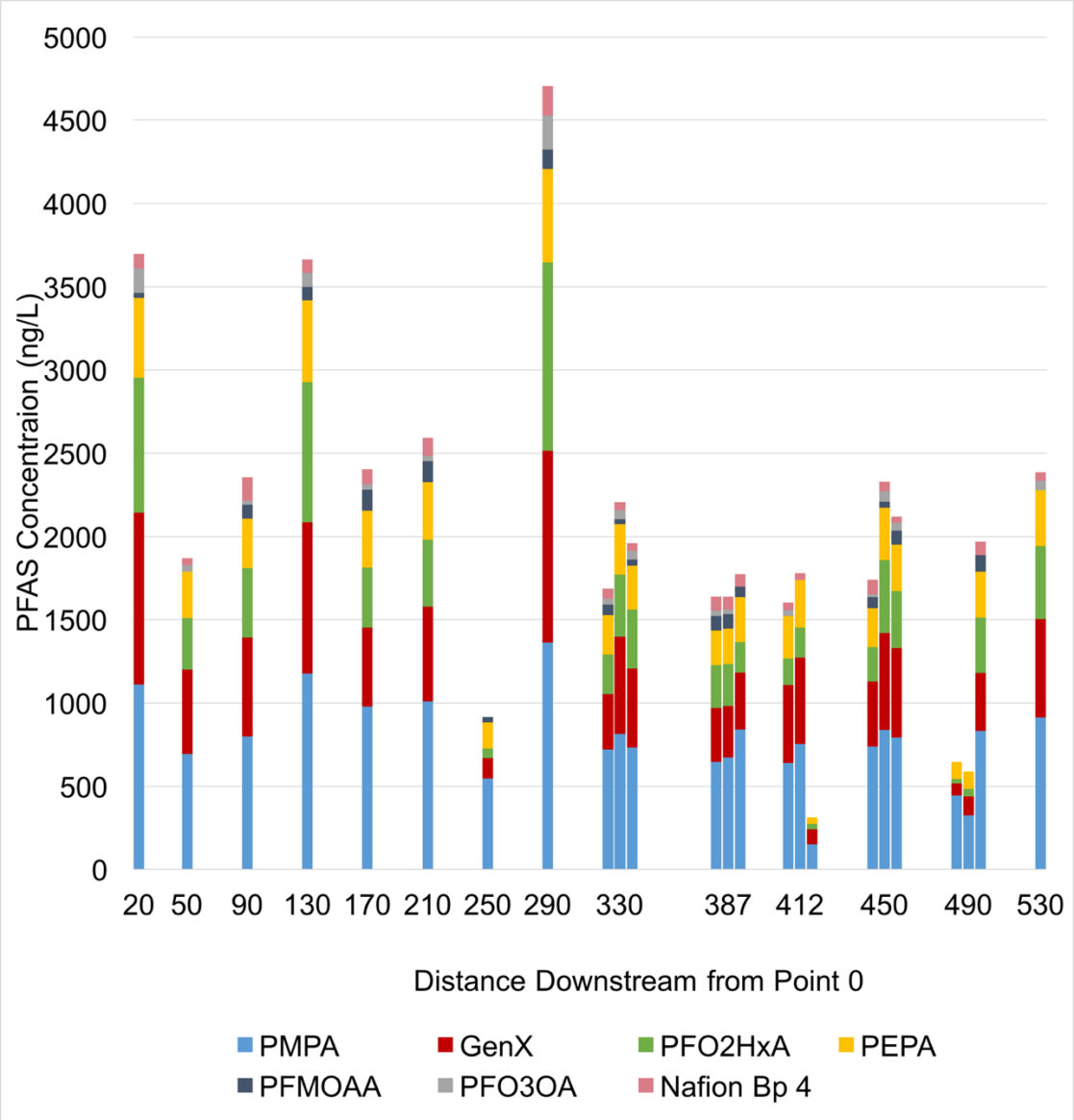

Figure 7. Total PFAS concentrations in groundwater at 24 points in/beneath the streambed of Georgia Branch. At each 3-point transect across the stream, the group of three bars shows, from left to right, the total PFAS concentrations at the left, center and right points. A point on the left side of the channel was not feasible at the 490 m transect, but measurements were made at 487L, and the PFAS data at 487L are plotted above as part of the 490 m transect.

Table 5. PFAS concentrations in groundwater at 24 points in/beneath the streambed of Georgia Branch and one surface water sample (GB387 SW). When the concentration was lower than the minimum reporting level (<5 ng L^{-1}), it was considered zero in calculations of total measured PFAS and average concentration of each PFAS. Two ** after a concentration represents a concentration that was above the highest calibration curve point and one * represents a sample injection where the peak area fell outside of the analytical window for that compound on the LC/MS and no concentration was reported by the lab.

Sampling Point	PFBA ($ng\ L^{-1}$)	PFPeA ($ng\ L^{-1}$)	PFHxA ($ng\ L^{-1}$)	PFHpA ($ng\ L^{-1}$)	PFOA ($ng\ L^{-1}$)	PFNA ($ng\ L^{-1}$)	PFDA ($ng\ L^{-1}$)	PFBS ($ng\ L^{-1}$)
GB20R	<MRL	14	<MRL	*	<MRL	<MRL	<MRL	<MRL
GB50C	<MRL	<MRL	<MRL	*	<MRL	<MRL	<MRL	<MRL
GB90L	<MRL	<MRL	<MRL	*	<MRL	<MRL	<MRL	<MRL
GB130C	<MRL	<MRL	<MRL	*	<MRL	<MRL	<MRL	<MRL
GB170L	<MRL	<MRL	<MRL	*	<MRL	<MRL	<MRL	<MRL
GB210C	<MRL	<MRL	<MRL	*	<MRL	<MRL	<MRL	<MRL
GB250R	<MRL	<MRL	<MRL	*	<MRL	<MRL	<MRL	<MRL
GB290C	25	19	<MRL	*	<MRL	<MRL	<MRL	<MRL
GB330L	<MRL	<MRL	<MRL	*	<MRL	<MRL	<MRL	<MRL
GB330C	<MRL	<MRL	<MRL	*	<MRL	<MRL	<MRL	<MRL
GB330R	<MRL	<MRL	<MRL	*	<MRL	<MRL	<MRL	<MRL
GB387L	<MRL	<MRL	<MRL	*	<MRL	<MRL	<MRL	<MRL
GB387C	<MRL	<MRL	<MRL	*	<MRL	<MRL	<MRL	<MRL
GB387R	26	<MRL	<MRL	*	<MRL	<MRL	<MRL	<MRL
GB412L	<MRL	<MRL	<MRL	*	<MRL	<MRL	<MRL	<MRL
GB412C	<MRL	<MRL	<MRL	*	<MRL	<MRL	<MRL	<MRL
GB412R	<MRL	<MRL	<MRL	*	<MRL	<MRL	<MRL	<MRL
GB450L	<MRL	<MRL	<MRL	*	<MRL	<MRL	<MRL	<MRL
GB450C	<MRL	<MRL	<MRL	*	<MRL	<MRL	<MRL	<MRL
GB450R	<MRL	<MRL	<MRL	*	<MRL	<MRL	<MRL	<MRL
GB490L	<MRL	<MRL	<MRL	*	<MRL	<MRL	<MRL	<MRL
GB490C	<MRL	<MRL	<MRL	*	<MRL	<MRL	<MRL	<MRL
GB490R	<MRL	<MRL	<MRL	*	<MRL	<MRL	<MRL	<MRL
GB530C	<MRL	<MRL	<MRL	*	<MRL	<MRL	<MRL	<MRL
GB387 SW	<MRL	<MRL	<MRL	*	<MRL	<MRL	<MRL	<MRL
Average	2.1	1.4	0.0	N/A	0.0	0.0	0.0	0.0
% of total	0.1	0.1	0.0	N/A	0.0	0.0	0.0	0.0

Table 5 (continued).

Sampling Point	PFPeS ($ng\ L^{-1}$)	PFHxS ($ng\ L^{-1}$)	PFHpS ($ng\ L^{-1}$)	PFOS ($ng\ L^{-1}$)	4:2 FTS ($ng\ L^{-1}$)	6:2FTS ($ng\ L^{-1}$)	NVHOS ($ng\ L^{-1}$)
GB20R	*	<MRL	<MRL	<MRL	<MRL	<MRL	<MRL
GB50C	*	<MRL	<MRL	<MRL	<MRL	<MRL	<MRL
GB90L	*	<MRL	<MRL	<MRL	<MRL	<MRL	<MRL
GB130C	*	<MRL	<MRL	<MRL	<MRL	<MRL	<MRL
GB170L	*	<MRL	<MRL	<MRL	<MRL	<MRL	<MRL
GB210C	*	<MRL	<MRL	<MRL	<MRL	<MRL	<MRL
GB250R	*	<MRL	<MRL	<MRL	<MRL	<MRL	<MRL
GB290C	*	<MRL	<MRL	<MRL	<MRL	<MRL	<MRL
GB330L	*	<MRL	<MRL	<MRL	<MRL	<MRL	<MRL
GB330C	*	<MRL	<MRL	<MRL	<MRL	<MRL	<MRL
GB330R	*	<MRL	<MRL	<MRL	<MRL	<MRL	<MRL
GB387L	*	<MRL	<MRL	<MRL	<MRL	<MRL	<MRL
GB387C	*	<MRL	<MRL	<MRL	<MRL	<MRL	<MRL
GB387R	*	<MRL	<MRL	<MRL	<MRL	<MRL	<MRL
GB412L	*	<MRL	<MRL	<MRL	<MRL	<MRL	<MRL
GB412C	*	<MRL	<MRL	<MRL	<MRL	<MRL	<MRL
GB412R	*	<MRL	<MRL	<MRL	<MRL	<MRL	<MRL
GB450L	*	<MRL	<MRL	<MRL	<MRL	<MRL	<MRL
GB450C	*	<MRL	<MRL	<MRL	<MRL	<MRL	<MRL
GB450R	*	<MRL	<MRL	<MRL	<MRL	<MRL	<MRL
GB490L	*	<MRL	<MRL	<MRL	<MRL	<MRL	<MRL
GB490C	*	<MRL	<MRL	<MRL	<MRL	<MRL	<MRL
GB490R	*	<MRL	<MRL	<MRL	<MRL	<MRL	<MRL
GB530C	*	<MRL	<MRL	<MRL	<MRL	<MRL	<MRL
GB387 SW	*	<MRL	<MRL	<MRL	<MRL	<MRL	<MRL
Average	N/A	0.0	0.0	0.0	0.0	0.0	0.0
% of total	N/A	0.0	0.0	0.0	0.0	0.0	0.0

Table 5 (continued).

Sampling Point	Nafion Bp1 (ng L^{-1})	Nafion Bp2 (ng L^{-1})	Nafion Bp4 (ng L^{-1})	PFO4DA (ng L^{-1})	PFO5DoA (ng L^{-1})	HydroEve (ng L^{-1})
GB20R	<MRL	25	88	*	<MRL	*
GB50C	<MRL	<MRL	42	*	<MRL	*
GB90L	<MRL	46	141	*	<MRL	*
GB130C	<MRL	18	81	*	<MRL	*
GB170L	<MRL	11	88	*	<MRL	*
GB210C	<MRL	14	109	*	<MRL	*
GB250R	<MRL	<MRL	<MRL	*	<MRL	*
GB290C	<MRL	22	179	*	<MRL	*
GB330L	<MRL	<MRL	61	10	<MRL	<MRL
GB330C	<MRL	17	50	*	<MRL	<MRL
GB330R	<MRL	13	45	*	<MRL	<MRL
GB387L	<MRL	12	85	<MRL	<MRL	<MRL
GB387C	<MRL	<MRL	76	<MRL	<MRL	<MRL
GB387R	<MRL	<MRL	76	<MRL	<MRL	<MRL
GB412L	<MRL	13	43	*	<MRL	*
GB412C	<MRL	<MRL	42	*	<MRL	*
GB412R	<MRL	<MRL	<MRL	*	<MRL	*
GB450L	<MRL	<MRL	88	*	<MRL	*
GB450C	<MRL	16	55	*	<MRL	*
GB450R	<MRL	13	35	15	<MRL	<MRL
GB490L	<MRL	<MRL	<MRL	<MRL	<MRL	<MRL
GB490C	<MRL	<MRL	<MRL	*	<MRL	*
GB490R	<MRL	<MRL	80	<MRL	<MRL	<MRL
GB530C	<MRL	17	51	*	<MRL	*
GB387 SW	<MRL	26	50	*	<MRL	*
Average	0.0	9.8	63	1.0	0.0	0.0
% of total	0.0	0.5	3.1	0.1	0.0	0.0

Table 5 (continued).

Sampling Point	PFMOAA (ng L^{-1})	PMPA (ng L^{-1})	PEPA (ng L^{-1})	GenX (ng L^{-1})	PFO2HxA (ng L^{-1})	PFO3OA (ng L^{-1})	Total conc. (ng L^{-1})
GB20R	31	1111**	479	1032**	809	147	3737
GB50C	<MRL	696	281	505	308	37	1870
GB90L	82	800	297	594	418	25	2403
GB130C	83	1177**	492	910	839	84	3682
GB170L	127	980	340	474	361	34	2414
GB210C	126	1010**	344	570	401	34	2608
GB250R	32	547	157	124	56	<MRL	916
GB290C	117	1365**	559	1151**	1131**	205	4773
GB330L	63	720	237	333	239	35	1699
GB330C	29	813	303	586	372	54	2224
GB330R	37	733	263	474	355	52	1972
GB387L	88	647	206	325	258	32	1653
GB387C	88	673	211	309	254	28	1638
GB387R	64	841	268	343	183	<MRL	1801
GB412L	<MRL	642	256	466	159	37	1615
GB412C	<MRL	753	286	522	178	<MRL	1780
GB412R	<MRL	151	38	91	33	<MRL	313
GB450L	66	740	235	389	206	18	1742
GB450C	37	838	315	583	436	64	2344
GB450R	84	794	281	536	342	47	2146
GB490L	<MRL	445	103	73	25	<MRL	646
GB490C	<MRL	326	104	114	44	<MRL	589
GB490R	99	832	276	348	335	<MRL	1970
GB530C	<MRL	915	333	590	439	58	2403
GB387 SW	<MRL	966	338	583	440	52	2454
Average	52.2	772.8	277.6	476.8	340.8	41.3	2039
% of total	2.6	37.9	13.6	23.4	16.7	2.0	100.0

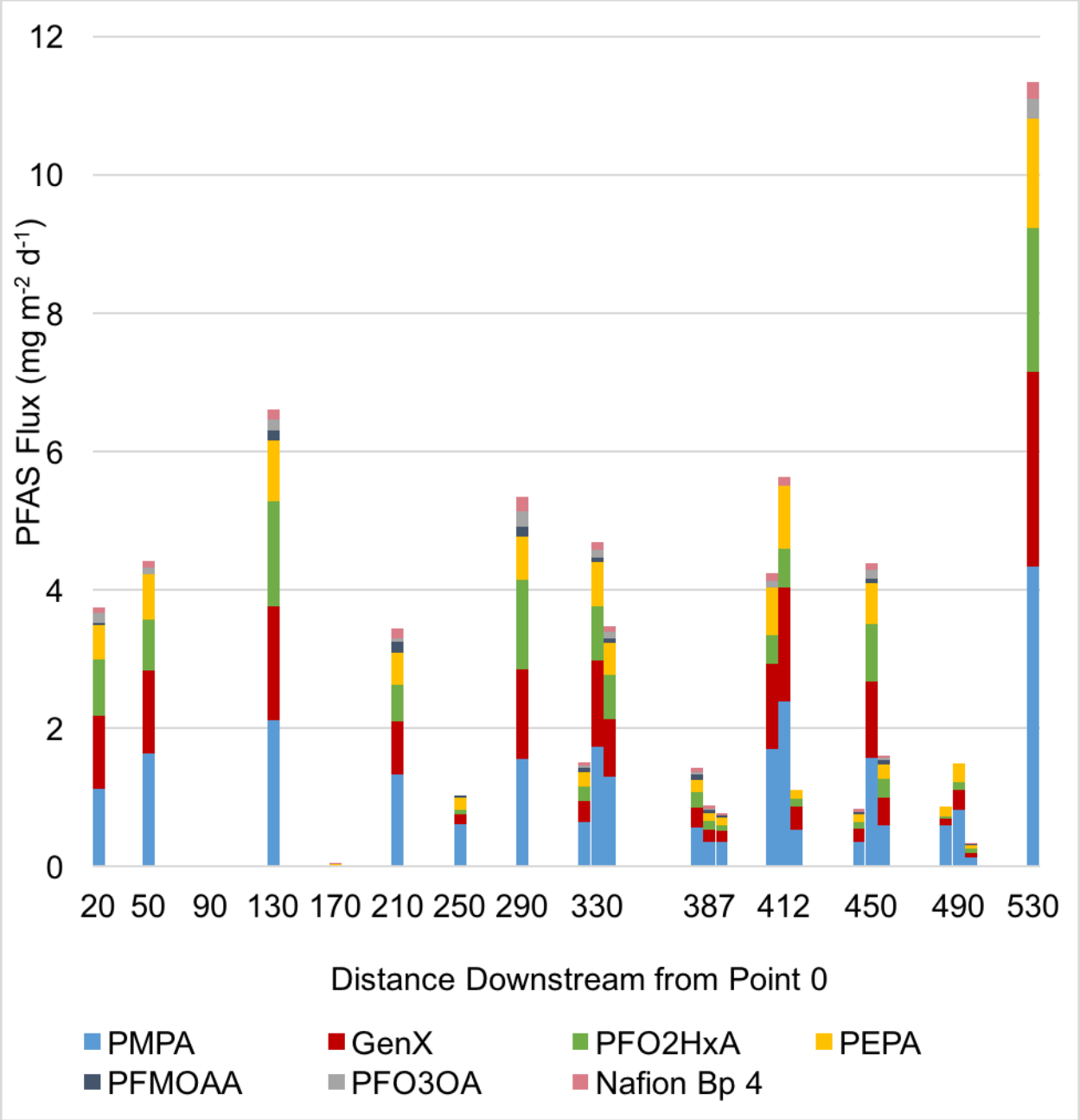

Figure 8. PFAS flux at 24 points in the streambed of Georgia Branch, February 2019. At each 3-point transect, the group of three bars shows, from left to right, the PFAS flux values at the left, center and right points. The 7 PFAS compounds shown make up 99.4% of the PFAS flux in Georgia Branch groundwater samples from February 2019. On average, PMPA, GenX, PFO2HxA, and PEPA together make up 93.3% of total PFAS flux.

Table 6. Streambed flux (groundwater to stream) of the 10 PFAS compounds present in groundwater samples, and total PFAS flux, in mg m^{-2} d^{-1}, at 24 points in the streambed of Georgia Branch, February 2019.

Sampling Point	PFO3OA (mg m^{-2} d^{-1})	PFBA (mg m^{-2} d^{-1})	PFPeA (mg m^{-2} d^{-1})	PFO4DA (mg m^{-2} d^{-1})	Nafion Bp2 (mg m^{-2} d^{-1})	Nafion Bp4 (mg m^{-2} d^{-1})
GB20R	0.150	<MRL	0.015	*	0.025	0.089
GB50C	0.088	<MRL	<MRL	*	<MRL	0.100
GB90L	0.000	<MRL	<MRL	*	0.000	0.001
GB130C	0.151	<MRL	<MRL	*	0.032	0.145
GB170L	0.001	<MRL	<MRL	*	0.000	0.001
GB210C	0.045	<MRL	<MRL	*	0.019	0.145
GB250R	<MRL	<MRL	<MRL	*	<MRL	<MRL
GB290C	0.232	0.029	0.022	*	0.025	0.203
GB330L	0.032	<MRL	<MRL	0.009	<MRL	0.055
GB330C	0.116	<MRL	<MRL	*	0.036	0.107
GB330R	0.093	<MRL	<MRL	*	0.023	0.080
GB387L	0.028	<MRL	<MRL	<MRL	0.011	0.074
GB387C	0.015	<MRL	<MRL	<MRL	<MRL	0.041
GB387R	<MRL	0.011	<MRL	<MRL	<MRL	0.033
GB412L	0.097	<MRL	<MRL	*	0.033	0.115
GB412C	<MRL	<MRL	<MRL	*	<MRL	0.132
GB412R	<MRL	<MRL	<MRL	*	<MRL	<MRL
GB450L	0.009	<MRL	<MRL	*	<MRL	0.042
GB450C	0.120	<MRL	<MRL	*	0.029	0.105
GB450R	0.036	<MRL	<MRL	0.011	0.010	0.027
GB490L	<MRL	<MRL	<MRL	<MRL	<MRL	<MRL
GB490C	<MRL	<MRL	<MRL	*	<MRL	<MRL
GB490R	<MRL	<MRL	<MRL	<MRL	<MRL	0.014
GB530C	0.277	<MRL	<MRL	*	0.080	0.244
Average flux	0.062	0.002	0.002	0.001	0.013	0.073
% of total flux	2.14	0.058	0.053	0.029	0.464	2.515

Table 6 (continued).

Sampling Point	PFMOAA	PMPA	PEPA	GenX	PFO2HxA	Total PFAS
	(mg m^{-2} d^{-1})	(mg m^{-2} d^{-1})	(mg m^{-2} d^{-1})	(mg m^{-2} d^{-1})	(mg m^{-2} d^{-1})	(mg m^{-2} d^{-1})
GB20R	0.032	1.128	0.487	1.048	0.821	3.705
GB50C	<MRL	1.644	0.663	1.194	0.728	4.317
GB90L	0.001	0.005	0.002	0.004	0.003	0.015
GB130C	0.149	2.122	0.886	1.640	1.512	6.491
GB170L	0.002	0.015	0.005	0.007	0.005	0.035
GB210C	0.167	1.340	0.457	0.757	0.532	3.315
GB250R	0.035	0.613	0.176	0.139	0.063	1.027
GB290C	0.132	1.549	0.634	1.307	1.285	5.216
GB330L	0.057	0.646	0.213	0.299	0.214	1.469
GB330C	0.061	1.729	0.644	1.244	0.792	4.620
GB330R	0.066	1.298	0.465	0.840	0.629	3.414
GB387L	0.077	0.565	0.180	0.284	0.225	1.370
GB387C	0.047	0.361	0.114	0.166	0.136	0.839
GB387R	0.028	0.364	0.116	0.149	0.079	0.747
GB412L	<MRL	1.699	0.677	1.233	0.421	4.161
GB412C	<MRL	2.384	0.907	1.652	0.562	5.638
GB412R	<MRL	0.539	0.136	0.324	0.117	1.117
GB450L	0.032	0.357	0.113	0.187	0.099	0.797
GB450C	0.070	1.580	0.593	1.099	0.822	4.312
GB450R	0.063	0.600	0.212	0.405	0.258	1.595
GB490L	<MRL	0.600	0.139	0.099	0.034	0.871
GB490C	<MRL	0.824	0.264	0.289	0.110	1.486
GB490R	0.017	0.142	0.047	0.059	0.057	0.322
GB530C	<MRL	4.345	1.582	2.805	2.085	11.174
Average flux	0.043	1.10	0.40	0.718	0.48	2.90
% of total flux	1.223	37.962	13.938	24.727	16.634	100.000

Table 7. The mean (μ), standard deviation (σ), and the coefficient of variation of PFAS concentration and flux of the 8 most abundant PFAS.

	Concentration			Flux		
PFAS Compound	**μ (ng L^{-1})**	**σ (ng L^{-1})**	**Coefficient of Variation**	**μ (ng L^{-1})**	**σ (ng L^{-1})**	**Coefficient of Variation**
PMPA	773	261	2.97	1.10	0.964	1.083
GenX	477	272	1.75	0.718	0.702	1.02
PFO2HxA	341	265	1.29	0.483	0.536	0.902
PEPA	278	119	2.33	0.	0.	
Nafion Bp 4	63.2	35.8	1.77	0.0730	0.0651	1.35
PFMOAA	52.2	32.8	1.59	0.0431	0.0482	1.264
PFO3OA	41.3	48.2	0.856	0.0620	0.0809	1.08
Nafion Bp 2	9.84	9.37	1.05	0.0135	0.0204	1.22
Total PFAS	2039	1001	2.04	2.90	2.69	1.08

7.3. Tritium-helium groundwater age dating results

The closed-system equilibration (CE) model (Aeschbach-Hertig et al., 2008) and noble gas data were used to estimate tritiogenic helium-3 concentrations in the groundwater samples. Apparent groundwater ages were calculated using the ratio of terrigenic helium-3 to tritium (Equation 1). For each point where an apparent groundwater age was calculated, the value of R/R_a was measured, where R is $[^3He]/[^4He]$ in the groundwater sample and R_a is the atmospheric $[^3He]/[^4He]$. R/R_a has a value of 0.98 for water equilibrated with modern air, so when R/R_a is near 1, the water sample appears to be in equilibrium with modern air (Solomon et al., 2010).

Only 3 out of 24 sampling points in Georgia Branch had tritium-helium age dates significantly above 0 years. These points are GB50C with an age of 14 years, GB412R with an age of 28 years, and GB490C with an age of 18 years.

The groundwater at GB412R had a much lower R/R_a and a higher concentration of ^4He (C_{GB412R}) than the other samples (Appendix A). Comparatively low R/R_a and high concentrations of ^4He are consistent with the mixing of PFAS-free old groundwater (high in ^4He) with younger

groundwater. In this context, "old" refers to groundwater much older than the tritium bomb peak (>69 years) that has elevated concentrations of ^{4}He derived from natural alpha decay of radioactive elements (mainly U, Th, Ra, Rn). When such mixing occurs between old and younger groundwaters, the tritium-helium age date of the mixture indicates the age of the young water, because Equation 1 is not affected by dilution with old groundwater with negligible tritium and tritiogenic ^{3}He (Schlosser et al., 1989).

To understand the extent to which mixing could be a factor at GB412R, a simple mixing model was applied to find the fraction of old water in the sample (f_{old}) using ^{4}He concentrations:

$$f_{\mathrm{old}} = \frac{C_{GB412R} - C_{young}}{C_{old} - C_{young}} \quad (2).$$

The concentration of ^{4}He in young groundwater (C_{young}) was the average ^{4}He concentration of the 21 groundwater samples with very young apparent ages. There were no local samples to represent old groundwater (C_{old}) in the mixing model, so I used a sample of Black Creek groundwater (from Well O30J1 in Saulston, NC, 111 km northeast of Georgia Branch) with a known ^{4}He concentration, from Kennedy and Genereux (2007). This old water was interpreted to be 425 years old (Kennedy and Genereux, 2007).

This simple mixing model shows that about 30% of the water in GB412R may be old water and 70% may be younger (28 years old). If 30% of the water sample at GB412R was 425 years old, the actual concentration of total PFAS in the sample would be 447 ng L^{-1} (313 ng per 0.7 L). This concentration of PFAS is much lower than the mean concentration (2039 ng L^{-1}), consistent with the interpretations of PFAS concentration and age in Section 7.4 below. Future investigations of groundwater in the Georgia Branch watershed should look at the issue of mixing between relatively young and older groundwater, using He or other naturally-occurring tracers, to understand the implications of potentially diluted PFAS concentrations.

21 of the 24 sampling points in Georgia Branch had R/R_a near 1, consistent with groundwater which may be zero to only a few years old (Solomon et al., 1996). One sample, GB387R, had higher He, Ne, Ar, and Kr concentrations than any of the other samples, most likely due to an air bubble accidentally captured in this sample during collection, resulting in a young apparent age that is more uncertain than those of the other samples with R/R_a near 1 (pers. comm., D.K. Solomon, Nov. 2019).

It is surprising to find groundwater at 21 of 24 sampling points with R/R_a near 1 and apparent ages near zero. The mean transit time (*MTT*) of these points was calculated as the flow-weighted mean apparent age of groundwater discharging from the streambed: $MTT = \Sigma v\tau/\Sigma v$, v is the specific discharge and τ is the apparent age of groundwater. *MTT* at Georgia Branch was 6.8 years, assuming an apparent age of 2.5 years for all groundwater samples with very young apparent ages (0-5 years). Other datasets collected with the same general approach in North Carolina and Wisconsin showed the *TTD* of groundwater in a surficial aquifer system to include a much smaller proportion of very young groundwater in the total groundwater discharged, compared to what was found in Georgia Branch (Fig. 9), and *MTT*s between 24 and 31 years [e.g., Browne and Guldan, 2005; Kennedy et al., 2009a,b; Gilmore et al., 2016a]. In these other datasets, only about 20% of the total groundwater discharging was very young water. Mechanisms that may explain the unusually high percentage (77%) of young groundwater (0-5 years old) discharging into Georgia Branch and the possibility that tritium-helium age dating is problematic at this site are explored in Section 8.

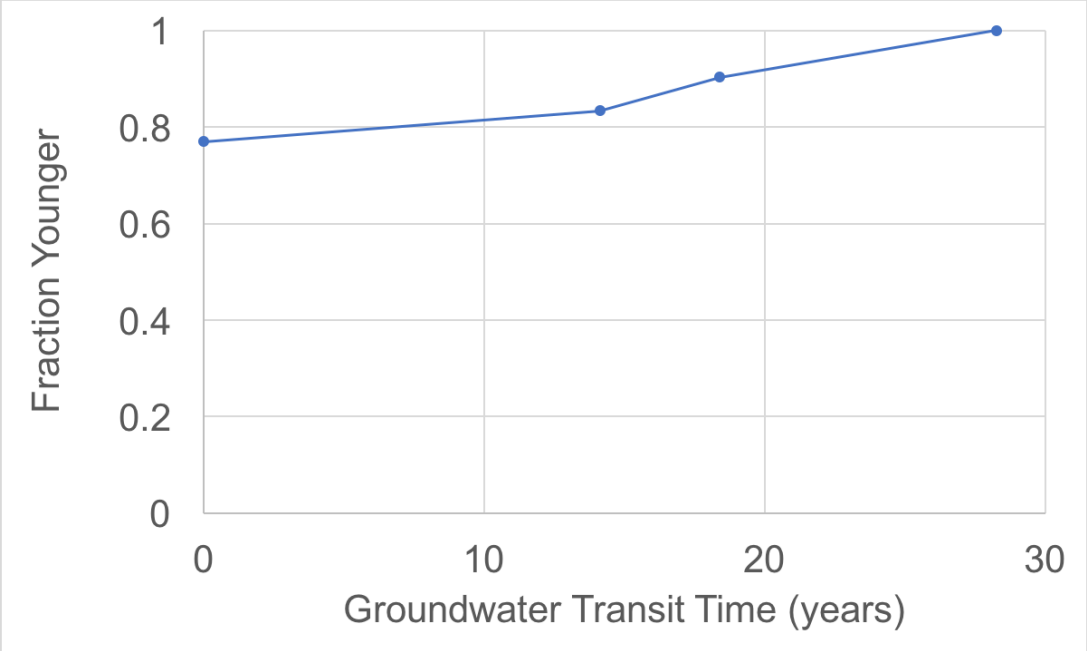

Figure 9. The transit time distribution of groundwater discharging at 24 points in the Georgia Branch stream channel. All of the discharge associated with the 21 streambed points with very young apparent age (0-5 years) was summed and plotted at zero transit time.

7.4. Concentration of PFAS and age of groundwater

There was a wide range of total PFAS concentrations in the groundwater with very young apparent ages (Figures 10-18). For the most abundant PFAS compounds, the mean concentration of groundwater with very young apparent ages was plotted with the concentrations of PFAS in the 3 samples with older apparent ages to give a graph with 4 points of PFAS concentration in groundwater plotted with apparent ages (Figure 19). Overall, there was a general decrease in PFAS concentration with increasing age, especially for the most abundant PFAS. The slopes were steepest between 14 and 18 years before sample collection (2001-2005), possibly indicating an increase in emissions during those years.

Figure 19 is based on only four points per each PFAS but suggests some insights beyond the general trend of decreasing concentrations with increasing age. PFAS concentrations of the four most abundant compounds (PMPA, GenX, PEPA, PFO2HxA) were significant in GB412R,

the oldest dated sample (28 years), even if the sample is diluted by 30% with pre-1950 groundwater (a possibility suggested by ^{4}He concentrations). The 28-year age of the GB412R sample, collected in 2019, implies the groundwater was recharged in 1991. The Chemours Company, formerly DuPont, acknowledged that the facility began emitting GenX in 1980 (Geosyntec, 2019a). If all PFAS emissions began in 1980, then Georgia Branch groundwater was significantly contaminated within at least 11 years (total PFAS = 313 ng/L in GB412R, a sample recharged in 1991), and possibly faster. Further data are needed to understand whether even older groundwater (older than 28 years) is significantly contaminated with PFAS; however, if the plant began operations in 1971, then groundwater with recharge dates before then should not have PFAS contamination.

Nafion Bp 4 and PFO3OA are absent in 18- and 28-year-old groundwater while Nafion Bp 2 and PFMOAA are both absent in the groundwater samples that are 14, 18, and 28 years old. It seems likely the lack of these four compounds in older groundwater is because the Chemours Company (formerly DuPont) began emitting these compounds later and/or at lower rates compared to the four most abundant PFAS. Another possibility to consider is whether the concentrations of these less abundant compounds (Nafion Bp 2, PFO3OA, Nafion Bp 4, PFMOAA) are lower because their transport through groundwater to the streams is retarded relative to the transport of the more abundant PFAS (PMPA, GenX, PEPA, PFO2HxA).

Retardation of PFAS in the saturated zone may affect the transit time of each compound. Geosyntec gives a median fraction of organic carbon (f_{oc}) equal to 0.0012 and median bulk density (ρ_b) of 1.5 kg L^{-1} for the surficial aquifer in the study area (Geosyntec, 2019a, p. 27). This bulk density implies a porosity of 0.43 if the density of solids is 2.65 g cm^{-3} (a typical density for quartz sand soils).

GenX has an organic carbon-water distribution coefficient (K_{oc}) of $10^{1.69}$ L kg^{-1}, derived by a linear free energy relationship from an experimental value of the GenX octanol-water partition coefficient (Geosyntec, 2019b). The values used by Geosyntec are similar to those predicted by models: log K_{oc} of GenX modeled by EPISuite 4.1 was 1.92 L kg^{-1} (Strynar et al., 2015) and log K_{oc} of PFMOAA and PFO2HxA were 0.68 L kg^{-1} and 0.70 L kg^{-1}, respectively (Comptox, 2019). Assuming linear reversible sorption controlled mainly by solid organic matter in the aquifer, a retardation factor (R) can be calculated as:

$$R = 1 + \frac{K_{oc} f_{oc} \rho_b}{n} \quad (3).$$

This approach to the calculation of R does not take into account retardation by mechanisms like ion exchange on charged surfaces, molecular diffusion into immobile zones, which has been documented for chemicals including volatile organic compounds and bromide in groundwater, or relatively weak adsorption by van der Waals' forces on mineral surfaces.

Estimated retardation factors are all close to 1 (Table 8). If the true retardation factors at the site are close to the estimated values, it suggests that the age-concentration relationship is mostly affected by the input rates to the surficial aquifer through atmospheric deposition rather than retardation. This implies that PMPA was input to the aquifer at a higher rate than GenX, which was input at a higher rate than PFO2HxA, etc. PFO2HxA may have had similar rates to PEPA, while other PFAS in Figure 19 probably had lower input to the groundwater. The fact that GenX has the second-highest retardation factor and is the second most abundant PFAS suggests that retardation may not be a major control on Figure 19 (i.e., that it's not a simple case of lower concentration due to higher R). Further work on the chemical properties of each PFAS and their retardation during transport would be necessary to fully clarify this relationship.

Table 8. Log K_{oc} values found by Geosyntec (2019b) using a linear free energy relationship between K_{ow} and K_{oc}, and experimental values of K_{ow}. Also shown are the estimated retardation factors of the eight most abundant PFAS at the study site.

PFAS	Log K_{oc} (L kg^{-1}) at pH 5	Retardation Factor
PMPA	1.02	1.04
GENX	1.69	1.21
PFO2HXA	1.17	1.06
PEPA	1.35	1.09
Nafion Bp 4	1.04	1.05
PFMOAA	0.89	1.03
PFO3OA	1.65	1.19
Nafion Bp 2	1.96	1.38

Water samples with low PFAS concentrations may indicate older groundwater. The two lowest concentration PFAS samples collected in the area around the Chemours Company by my research group were collected beneath Willis Creek, a tributary to the Cape Fear River that is 4.4 km north of Georgia Branch, in August 2018: the Willis Creek 2 sample had 20 ng L^{-1} of PMPA and no other PFAS, and the Willis Creek 1 sample had only 89 ng L^{-1} PMPA and 13 ng L^{-1} PEPA (Koropeckyj-Cox, 2019).

If PFAS concentrations do decrease with age, then Willis Creek 2 may be the oldest groundwater sample has been found so far near the Chemours Company. No groundwater samples without any PFAS contamination have been found in this work or earlier work at the same field site (Koropeckyj-Cox 2019). The Willis Creek 2 sample may represent the leading edge of PFAS "breakthrough" at the Willis Creek streambed (i.e., the first arrival of PFAS at that spot on the streambed). Willis Creek 2 groundwater is probably not older than 48 years, as the Fayetteville Works began operations in 1971, so 1971 is the earliest year that PFAS could have been emitted (DuPont, 2002). If there were significant PFAS travel time in the unsaturated zone before reaching the water table, then the Willis Creek 2 groundwater sample would be younger

than 48 years (e.g., if there were 10 years of travel time in the unsaturated zone, then groundwater age could be 38 years rather than 48 years).

In Georgia Branch, no groundwater without contamination has been found; therefore, no groundwater has been found that can reasonably be assumed to be older than the source of contamination (48 years at most, considering 2019 sampling in Georgia Branch and 1971 as the start of PFAS emission). Also, the oldest of the 24 age-dated Georgia Branch groundwater samples was 28 years old and significantly contaminated. While 3-4 points are not adequate to construct a full groundwater *TTD* with confidence (Fig. 9), the lack of old and uncontaminated groundwater suggests that there may be a relatively low mean transit time (*MTT*) in the watershed. A greater groundwater *MTT*, or longer tail toward old ages on the *TTD*, could be expected if there were many samples of groundwater containing no PFAS. A possible exception to this lack of old water may be inferred from one analyte in one sample (GB412R) with elevated helium-4 concentration, discussed in Section 7.3.

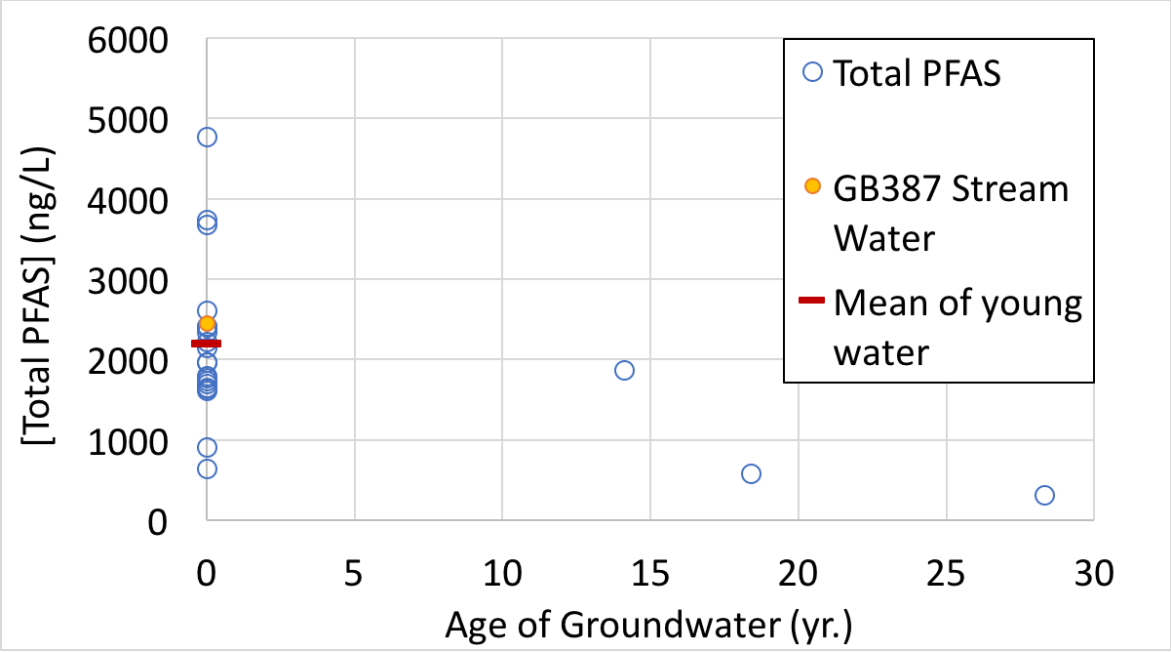

Figure 10. The relationship between total PFAS concentration and groundwater age at 24 points in Georgia Branch. Groundwater samples of very young apparent age (0-5 years), and stream water from GB387, are plotted at zero age.

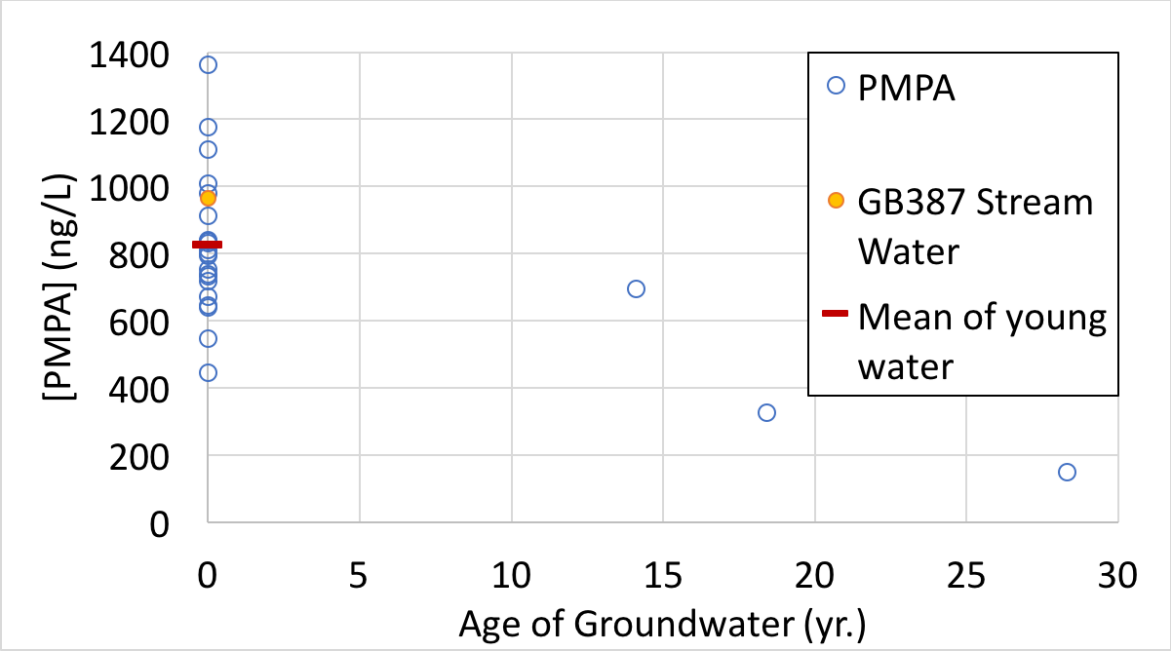

Figure 11. The relationship between PMPA concentration and groundwater age at 24 points in Georgia Branch. Groundwater samples of very young apparent age (0-5 years), and stream water from GB387, are plotted at zero age.

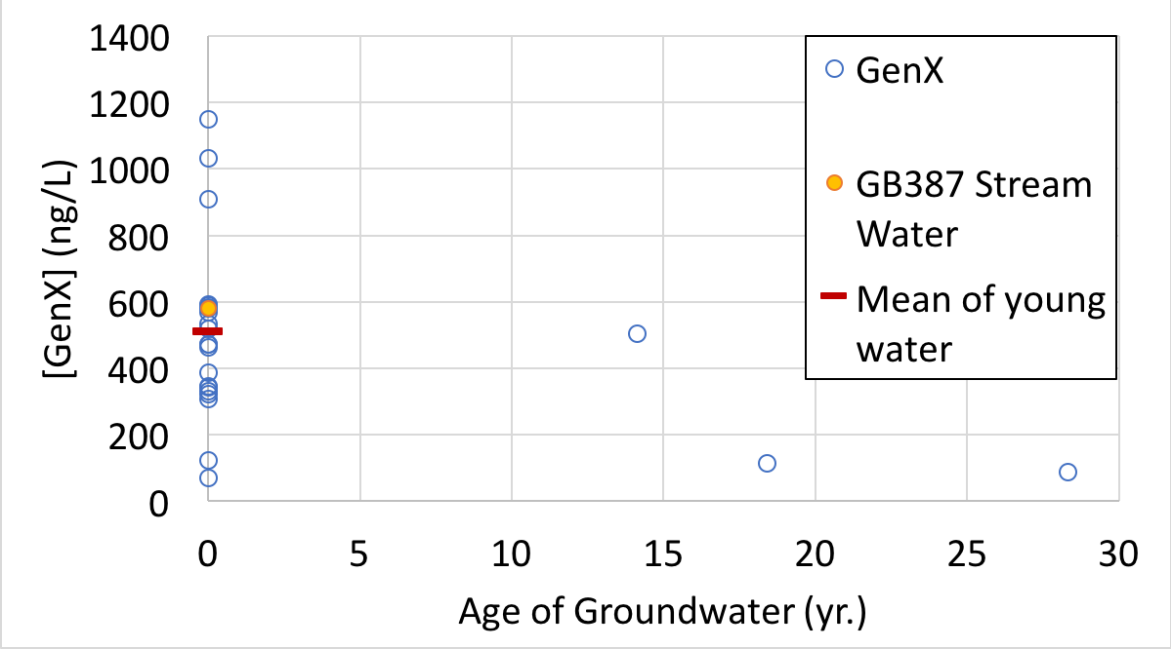

Figure 12. The relationship between GenX concentration and groundwater age at 24 points in Georgia Branch. Groundwater samples of very young apparent age (0-5 years), and stream water from GB387, are plotted at zero age.

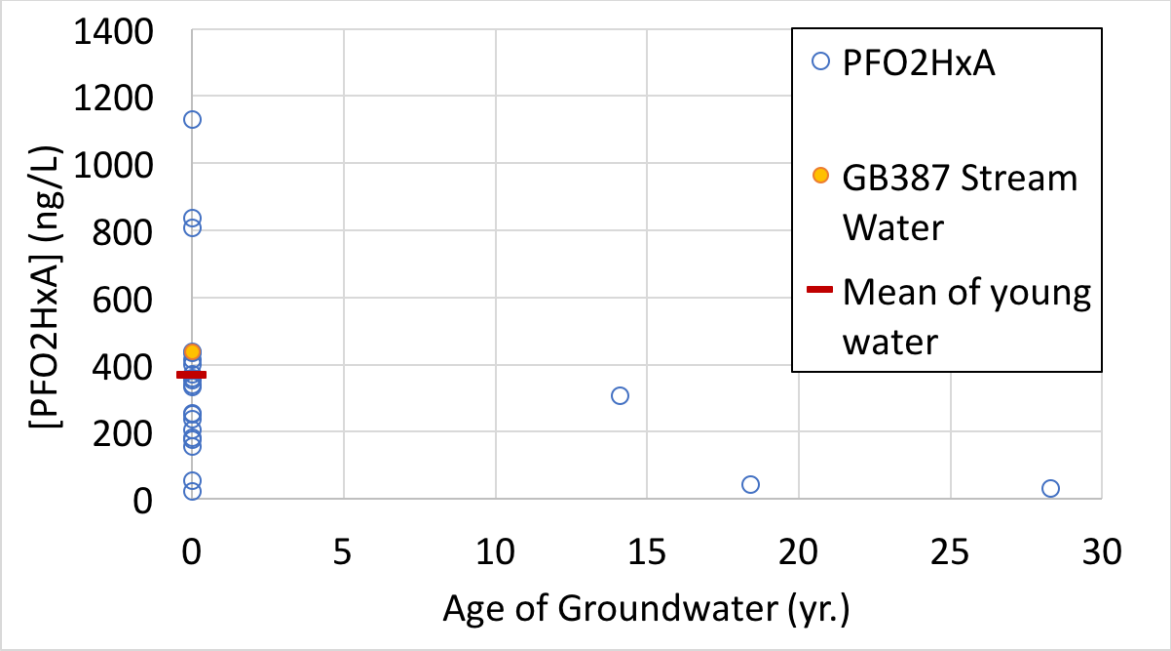

Figure 13. The relationship between PFO2HxA concentration and groundwater age at 24 points in Georgia Branch. Groundwater samples of very young apparent age (0-5 years), and stream water from GB387, are plotted at zero age.

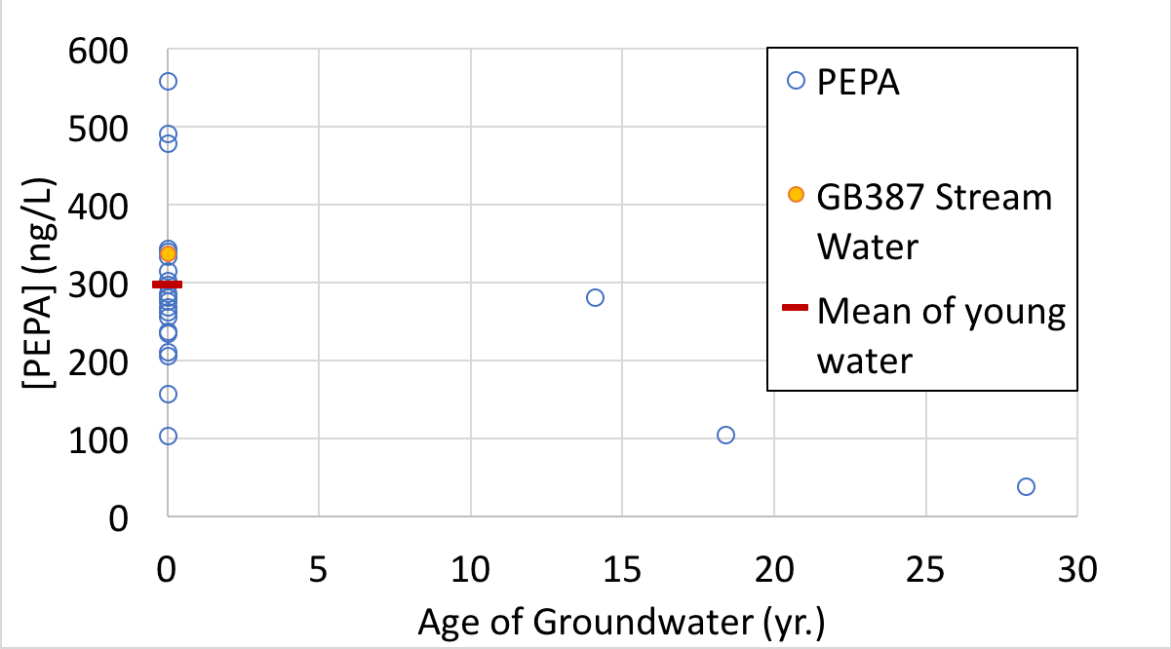

Figure 14. The relationship between PEPA concentration and groundwater age at 24 points in Georgia Branch. Groundwater samples of very young apparent age (0-5 years), and stream water from GB387, are plotted at zero age.

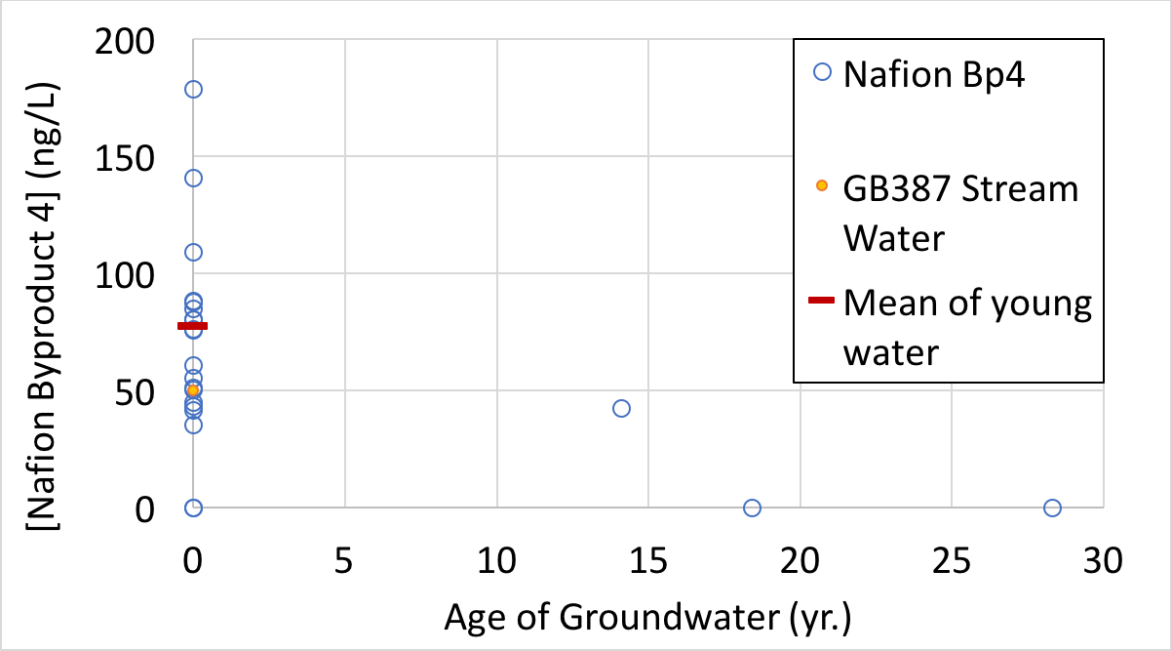

Figure 15. The relationship between Nafion Byproduct 4 concentration and groundwater age at 24 points in Georgia Branch. Groundwater samples of very young apparent age (0-5 years), and stream water from GB387, are plotted at zero age.

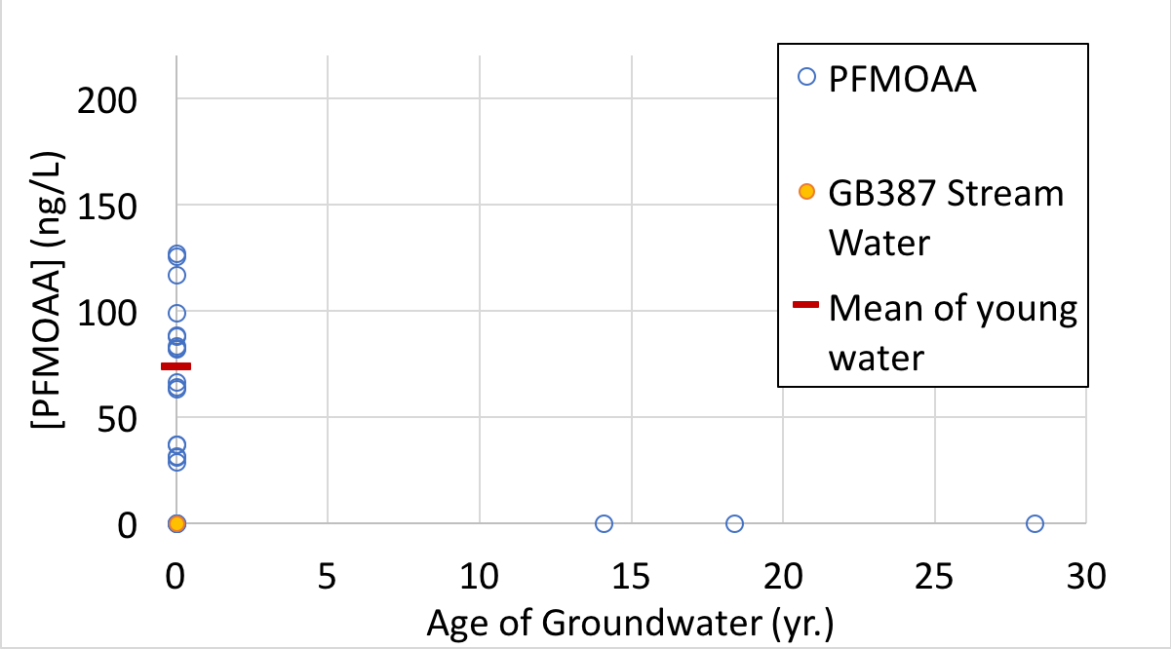

Figure 16. The relationship between PFMOAA concentration and groundwater age at 24 points in Georgia Branch. Groundwater samples of very young apparent age (0-5 years), and stream water from GB387, are plotted at zero age.

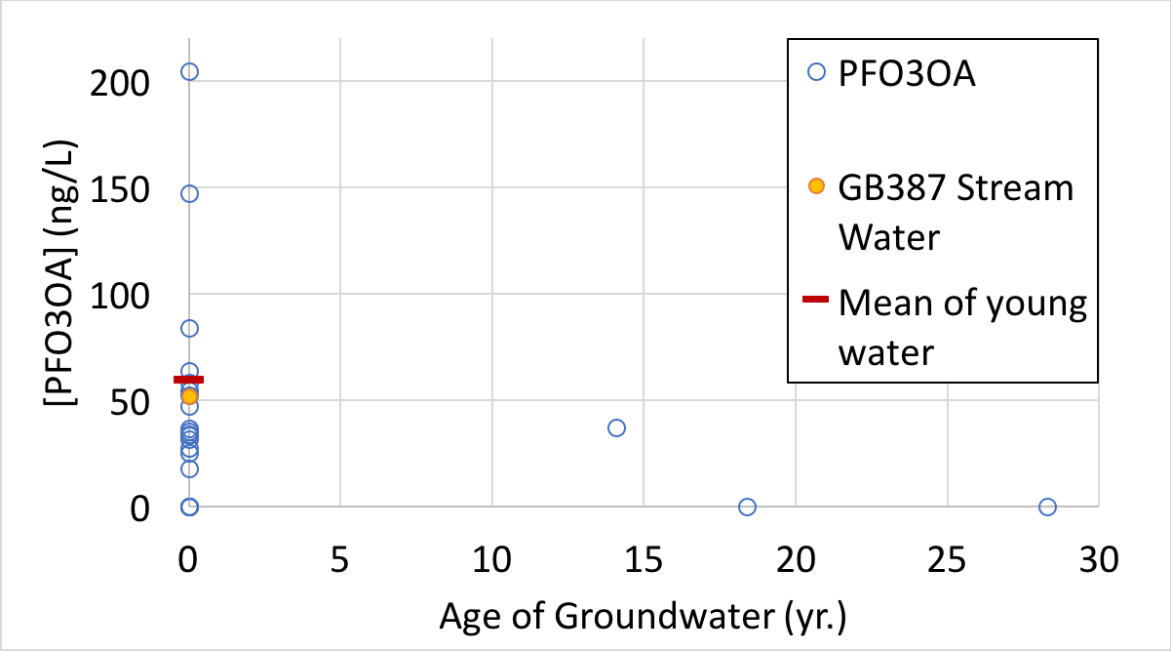

Figure 17. The relationship between PFO3OA concentration and groundwater age at 24 points in Georgia Branch. Groundwater samples of very young apparent age (0-5 years), and stream water from GB387, are plotted at zero age.

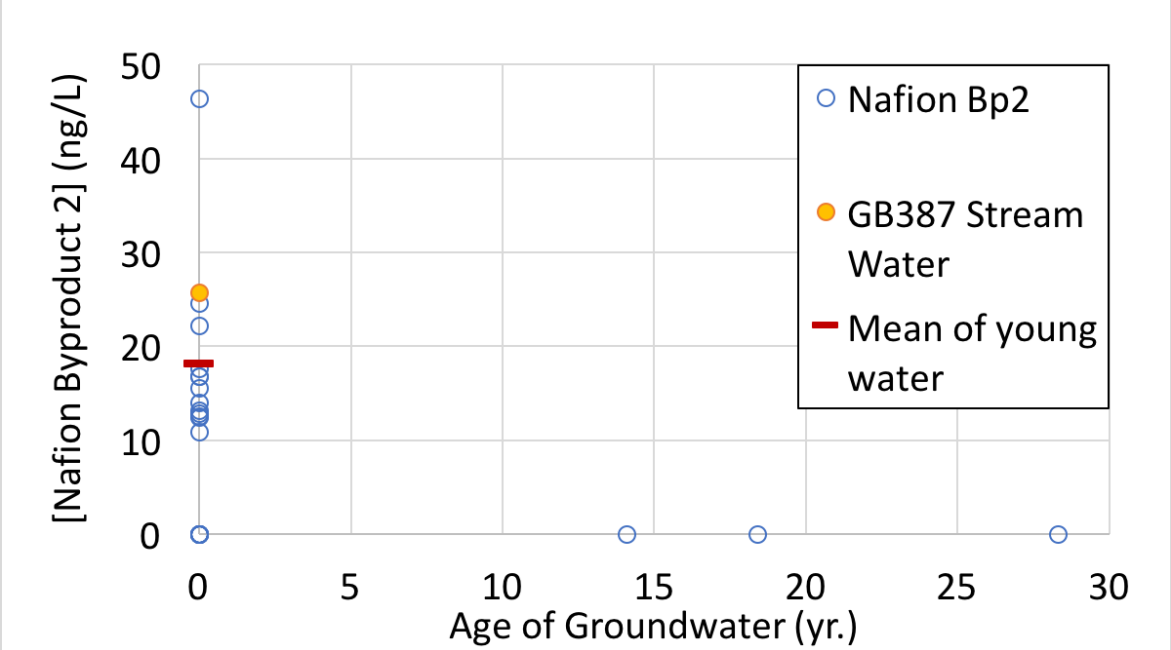

Figure 18. The relationship between Nafion Byproduct 2 concentration and groundwater age at 24 points in Georgia Branch. Groundwater samples of very young apparent age (0-5 years), and stream water from GB387, are plotted at zero age.

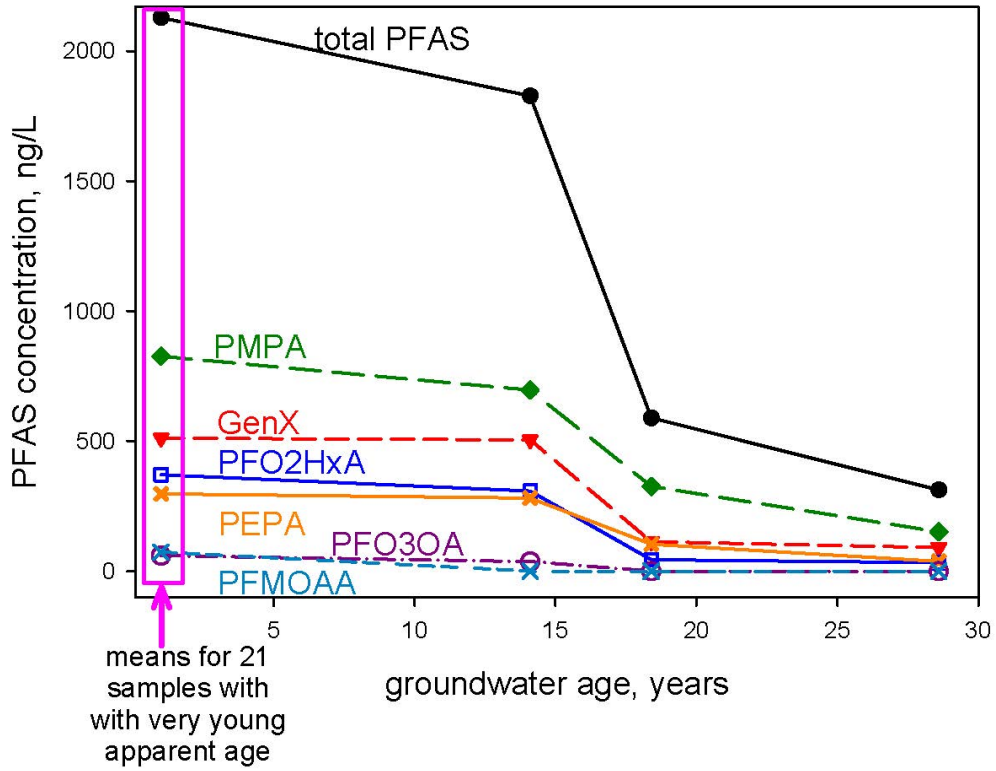

Figure 19. The relationship between groundwater age and PFAS concentration. Groundwater samples of very young apparent age (0-5 years) are plotted at zero age. Figure from D. P. Genereux.

Finally, as a rough check on the timeline for groundwater contamination with PFAS at the study site, extrapolation of the PFAS concentration trends defined by the two oldest groundwater samples was used to generate a crude estimate of the earliest year in which groundwater was contaminated by PFAS emissions to air at the Fayetteville Works (Figure 20). Results were 1979 for total PFAS, 1982 for PMPA, 1985 for PEPA, and 1950 for GenX. While the estimate for GenX is unrealistic, because it predates the start of operations at the plant (1971), the other three estimates seem plausible based on what is known. They each fall after 1971, and after or within a year of 1980 (the earliest year for which the Chemours Company acknowledges GenX emission from the plant), and the estimate for PMPA slightly precedes the estimate for PEPA, consistent with the suggestion from the Willis Creek 1 and 2 groundwater samples that PMPA emissions began before PEPA emissions.

This analysis may be performed more accurately with additional data on groundwater age and PFAS concentration in future studies. The analysis shown here is only a simple linear extrapolation based on two points per curve, for total PFAS and three of the most abundant individual PFAS. These simple extrapolations illustrate the concept and provide some results that are not unreasonable in light of current knowledge and data.

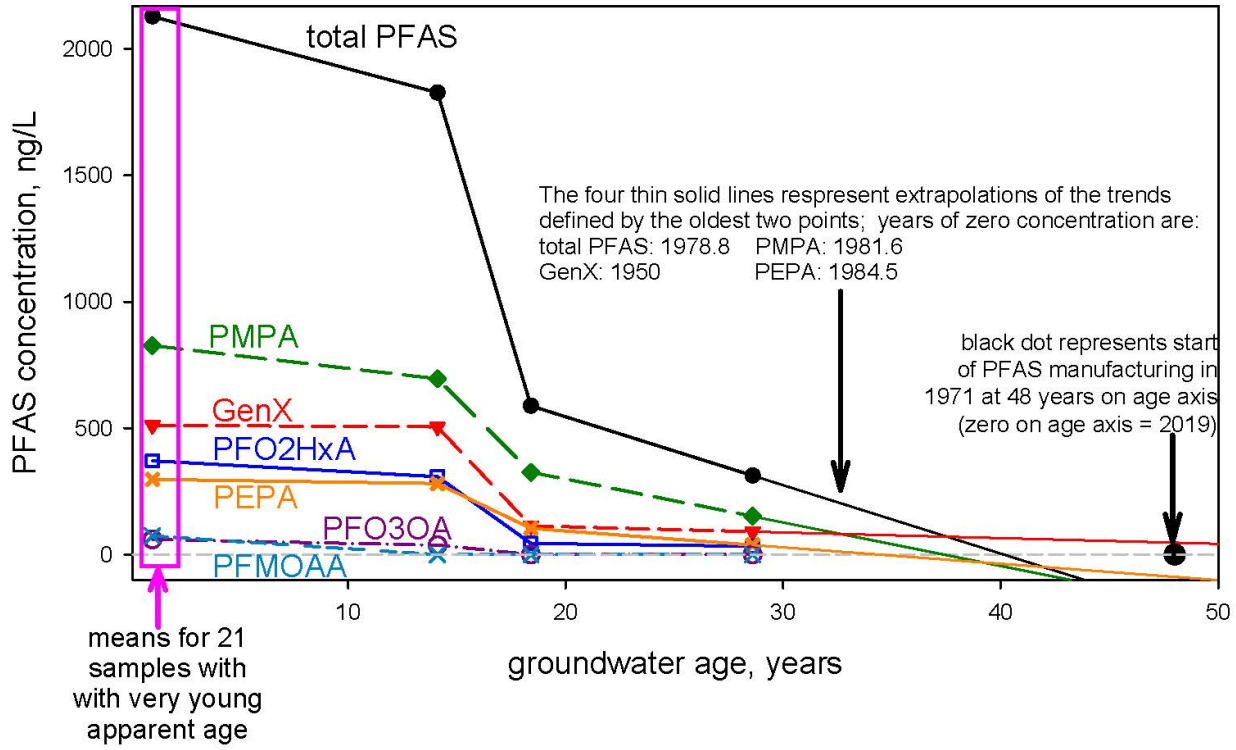

Figure 20. PFAS concentration and groundwater age, with extrapolations back in time for total PFAS, PMPA, GenX, and PEPA, based on linear trends for each defined by the two oldest age-dated groundwater samples (18 and 28 years old). Extrapolating back to zero concentration provides a crude estimate of the year of earliest groundwater contamination. Only the estimate for GenX is not possible (it predates the start of operations at the plant in 1971); the estimates for total PFAS, PMPA, and PEPA fall between 1979 and 1985, which may be plausible considering the 1971 start date for the plant (1980 is the earliest year for which Chemours acknowledges that GenX was released to air at the manufacturing plant). In principle, the year of earliest groundwater contamination should post-date the first year of PFAS emission to air by a lag time associated with the PFAS transport time through the unsaturated zone. Figure by D. P. Genereux.

7.5. PFAS transit time distribution

Groundwater *TTD* is evaluated by plotting the cumulative fraction of groundwater discharge as a function of groundwater age (Fig. 9). In the same way that a groundwater *TTD* plot shows the fraction of groundwater discharging that is younger than a certain age, a chemical *TTD* would show the fraction of a chemical discharging to a stream through groundwater that is younger than a certain age. This chemical *TTD* is plotted by having paired chemical flux and groundwater age data (i.e., values of groundwater age and chemical flux from groundwater to a stream at the same points on a streambed), and then plotting the cumulative fraction of chemical flux against the groundwater age.

A *TTD* curve for an individual PFAS compound would show the fraction of the individual PFAS flux that is younger than a certain age. This *TTD* would hypothetically mirror the *TTD* of groundwater if there were no significant PFAS retardation and if the contamination was occurring over a long enough time with a steady input rate, so that all the groundwater contained the same concentration of that individual PFAS. The latter does not seem to be the case in Georgia Branch; there was a wide range of PFAS concentrations in groundwater (Figs. 10-19), but the PFAS *TTD*s looked very similar to that of the groundwater itself (Fig. 9).

The *TTD*s of total PFAS and GenX reflect the finding that 90% of the discharge of each from the aquifer to Georgia Branch occurred in groundwater of very young apparent age (Figs. 20, 21). 100% of the total PFAS flux occurred in groundwater 28 years old or less (the age of the oldest groundwater dated from the February 2019 sampling campaign).

It seems surprising that 90% of total PFAS flux and GenX flux happens through groundwater with very young age dates. Section 8 discusses at least one hydrologic mechanism by which this might have happened, based on short groundwater flow paths from the riparian

area to the streambed. The concept of a chemical transit time distribution would be worth exploring with future data collection that includes more age dated groundwater and, perhaps, different sampling locations and age dating tracers.

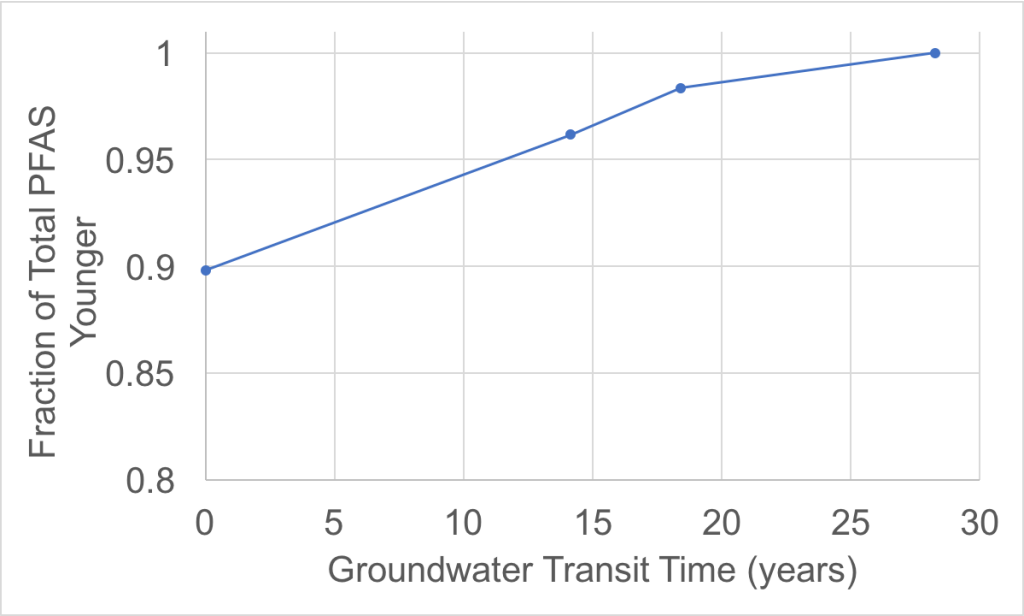

Figure 21. The transit time distribution of total PFAS discharging from groundwater at 24 points in the Georgia Branch stream. All PFAS discharge associated with groundwater of very young apparent age (0-5 years) is accounted for in the point plotted at zero age.

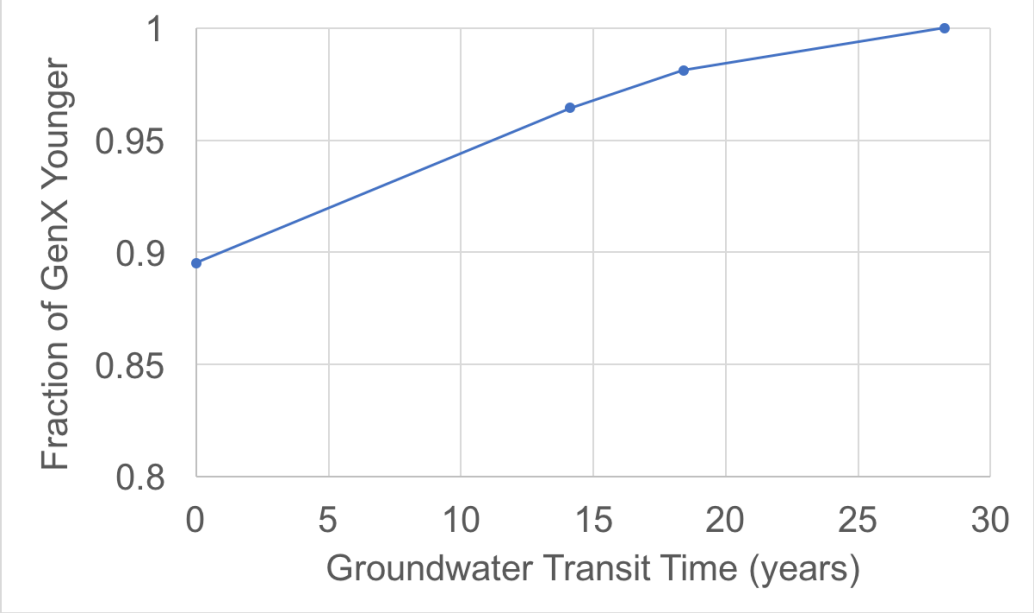

Figure 22. The transit time distribution of GenX discharging from groundwater at 24 points in the Georgia Branch stream. All GenX discharge associated with groundwater of very young apparent age (0-5 years) is accounted for in the point plotted at zero age.

8. Mechanisms that may affect tritium-helium age dating

8.1. The Age Dating Puzzle

The Georgia Branch *TTD* was markedly different from the *TTD* determined at West Bear Creek, about 110 km north in the Neuse River watershed (Gilmore et al., 2016a). Through initial sampling campaigns and observations at Georgia Branch, the site seemed similar to West Bear Creek where the same streambed methods applied in Georgia Branch were successful in defining the *TTD* of discharging groundwater. It was unexpected that the tritium-helium age dating results showed such a high proportion of very young groundwater discharging into Georgia Branch when compared to previous studies (Browne and Guldan, 2005; Kennedy et al., 2009a,b; Gilmore et al., 2016a). At West Bear Creek, and a site in Wisconsin (Browne and Guldan, 2005), *TTD*s were reasonably well described by a gamma function, with most of the groundwater discharge (about 70%) comprised of groundwater 20 to 40 years old, and the remaining amount (30%) equally split between groundwater younger than 20 years and older than 40 years.

This section discusses different hydrologic mechanisms that could be responsible for the widespread groundwater of very young apparent age (0-5 years) in the Georgia Branch streambed; the mechanisms discussed suggest that the tritium-helium age dates from Georgia Branch are either consistent with a broad occurrence of truly young groundwater discharge to the streambed, or that there was a complication with the application of tritium-helium age dating at the site.

8.2. Sampling errors

The errors in groundwater ages for the Georgia Branch samples, as calculated using the International Atomic Energy Agency's iNOBLE v.2.2, were usually 1-3 years. Sampling errors

in the field could affect tritium-helium age dating of groundwater. Bubbles of modern air in groundwater samples used for tritium-helium dating can significantly change the concentrations of He and other noble gases measured in each sample. Only one sample was assessed by the University of Utah Noble Gas Laboratory as having significant excess air, judging by neon concentration (GB387R). The groundwater samples for noble gas analysis were collected in copper tubes, and if the ends of the copper tubes were not perfectly sealed by the clamps, then the concentration of helium-3 measured could be significantly affected. Issues with clamps are unlikely in these samples. The clamped tubes were subjected to a leak check at the lab before testing, and no issues were found with any of the Georgia Branch samples (pers. comm., D.K. Solomon, Nov. 2019).

8.3. Sampling in the hyporheic zone

The hyporheic zone represents an area where surface water and groundwater mix in the streambed. Hyporheic circulation occurs when stream water cycles through a streambed, entering the bed in one location and exiting downstream. With strong hyporheic circulation, it could be possible that the water sampled through piezometers that were placed 35 cm into the streambed represents stream water or a mix of stream water and groundwater. It is likely that stream water would have R/R_a close to 1. Stream water traveling through the hyporheic zone is not expected to remain there for a long enough time that its R/R_a would change from 1.

In order for this mechanism to explain the noble gas data and age estimates from Georgia Branch, hyporheic circulation would need to be strong and extensive enough to make up the majority of water sampled for at least 21 out of 24 points. The PFAS concentrations in the water samples from all 21 points would have to be very similar to those of the stream water sample,

which was not the case. There was a wide range of PFAS concentrations among the 21 water samples with young apparent ages, with most significantly different from that of the stream water sample (Figs. 10-19). All point measurements occurred at streambed locations with an upward flow of groundwater and not downward flow. It is extremely unlikely that, if there were significant hyporheic circulation (which is initiated by the downward flow of stream water into the streambed), that all 24 sampling points would have been only in areas where stream water was exiting the streambed.

8.4. Diffusive fractionation of ^{3}H and tritiogenic ^{3}He

Interbedded sand layers between clay layers could provide preferential flow paths for water in the surficial aquifer and the Black Creek Confining Unit (Fig. 23). In a heterogeneous medium, such as shown in Fig. 23, diffusive fractionation of ^{3}H and ^{3}He may change the ^{3}H/^{3}He ratio so that groundwater in sand layers appears younger than it is (LaBolle et al., 2006). The aqueous phase molecular diffusion coefficient for ^{3}He is 3 to 4 times the coefficient of ^{3}H (LaBolle et al., 2006); therefore, ^{3}He may diffuse from high *K* sand layers to low *K* clay layers much more quickly than the diffusion of ^{3}H would occur, changing the ratio of ^{3}H/^{3}He in the sand layers and giving the appearance of younger groundwater in the sand.

LaBolle et al. (2006) concluded that this phenomenon may have a significant effect on tritium-helium age dating for groundwater recharged during the rising limb of the ^{3}H bomb peak (1950-1963). This would represent 56-69 year old groundwater in 2019. The apparent age of the oldest groundwater collected at Georgia Branch is only 28 years, suggesting it entered the saturated zone in 1991. As PFAS likely entered groundwater in this area no earlier than 1971 (48 years before 2019) and no groundwater without PFAS has been sampled in Georgia Branch,

discharge at Georgia Branch is probably not old enough to have groundwater from the ^{3}H bomb peak. This mechanism is unlikely to have significantly affected the $^{3}H/^{3}He$ ratio and R/R_a of the fairly young groundwater discharging into Georgia Branch.

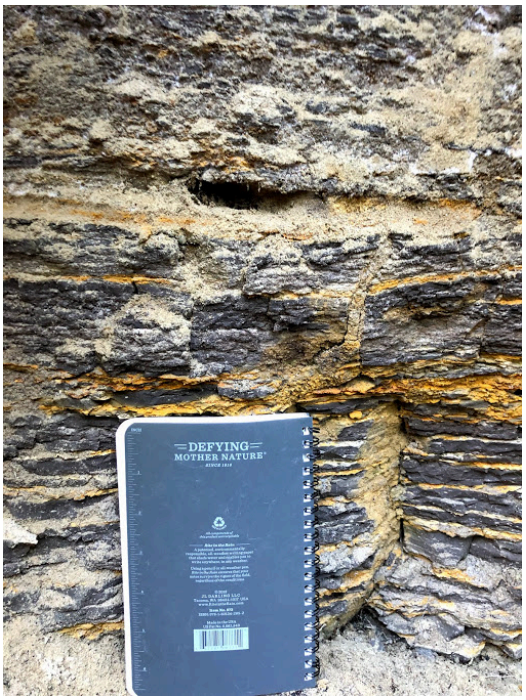

Figure 23. Interbedding of sand and clay layers along the western bank of Georgia Branch about 30 m downstream of the zero point.

8.5. The Low Recharge Rate Mechanism: Loss of tritiogenic ^{3}He at the water table due to low recharge rate

The loss of tritiogenic ^{3}He by gas exchange at the water table is possible, in theory, under a very low groundwater recharge rate, about 3 cm yr^{-1} or less (Solomon and Cook, 2000). The loss of tritiogenic ^{3}He would change the $^{3}H/^{3}He$ ratio and generate an R/R_a close to 1, suggesting a younger apparent age than the actual age of the groundwater.

North Carolina Coastal Plain sites are generally expected to experience an average recharge rate of at least 20-25 cm yr^{-1} (Gilmore et al., 2016a). A 2005 model by the USGS estimated a slightly higher range of recharge rates in the region, 25-40 cm yr^{-1} (USGS, 2005). A

crude estimate of recharge was determined by dividing base flow discharge (Q) in Georgia Branch by the area of the basin upstream of the discharge measurement point (A). The estimated recharge rate for Georgia Branch, using discharge estimates measured by injecting a salt solution to the stream, ranged throughout the year from 18 cm yr^{-1} (Q = 0.106 m^3 s^{-1}) in December 2019 to 54.9 cm yr^{-1} (Q = 0.324 m^3 s^{-1}) in February 2020. The range of these estimated recharge values suggests that the recharge value is large enough to allow for the retention of tritiogenic ^3He in a homogeneous hydrogeological system (Schlosser et al., 1989).

Hydrogeological observations, at the field site and in the region, suggest the hydrogeology is more complicated than a homogeneous sandy surficial aquifer. Geosyntec (2019c, p.16) drilled numerous boreholes at the Fayetteville Works and observed a perched saturated zone above a shallow clay layer roughly 5 m deep in the surficial aquifer. Drainage of the perched saturated zone creates seeps and streams that are elevated above the regional water table that lies deeper in the surficial aquifer. An unsaturated zone is located between the perched saturated zone and the regional water table (Geosyntec 2019a).

Geosyntec observed four groundwater seeps onsite at the Fayetteville Works and at least 10 more offsite along the western side of the Cape Fear River, between where Old Outfall 002 and Georgia Branch empty to the river (Geosyntec, 2019a, p. 21). These seeps are groundwater-fed from the perched saturated zone where the shallow clay layer in the surficial aquifer intersects the ground surface along bluffs and steep slopes. Field observations at Georgia Branch confirm that some small seeps can be found on the hillslope where the shallow clay layer intersects the ground surface. A small seep was observed on the left side of the stream at GB50 in November 2019, and two seeps were observed on the right and left sides of the stream, high above it, between GB570 and GB610.

Recharge to the base of the surficial aquifer, below the perched saturated zone, may be significantly reduced by this shallow clay layer. If a significant amount of recharge is captured by the perched saturated zone above the shallow clay and routed laterally from there to seeps and small streams that originate high on the hillslopes where the shallow clay intersects the ground surface, then the recharge reaching the regional water table in the lower part of the surficial aquifer may be greatly reduced.

In that case, groundwater in the lower part of the surficial aquifer (the likely source of water to the sampling locations in the Georgia Branch streambed) may experience the loss of tritiogenic ^{3}He due to the reduced recharge rate and, therefore, have R/R_a values close to 1. This groundwater may also have a wide range of ages and recharge years (even if the $^{3}H/^{3}He$ ages are all small), and thus a wide range of PFAS concentrations. If the loss of ^{3}He was widespread enough that the majority of the sampling points were discharging seemingly young groundwater due to lack of retention at the water table, then this mechanism would indicate an issue with the application of tritium-helium age dating at the study site. Groundwater with young apparent ages due to the loss of tritiogenic ^{3}He but a large range of PFAS concentrations, as found here, would be consistent with this mechanism (Figs. 10-18).

8.6. The Re-infiltration Mechanism: Re-infiltration of groundwater exfiltrated from the perched saturated zone

Groundwater from the perched saturated zone was observed seeping out of the ground (exfiltrating) along the hillslope surrounding Georgia Branch and along the western banks of the Cape Fear River (Geosyntec, 2019a, p. 21, 64). As exfiltrated water from the perched saturated zone runs downslope toward the riparian area of the perennial stream, it would lose tritiogenic

^{3}He by gas exchange and R/R_a would likely increase to 1. If this water then re-infiltrates on the lower slopes and riparian area near the Georgia Branch stream, it would likely follow a relatively short flowpath through the aquifer to the streambed of Georgia Branch, arriving there with R/R_a near 1 and a very young $^{3}H/^{3}He$ age.

A different process related to topography, and not the perched saturated zone, may produce the same result of focused re-infiltration in riparian areas following exfiltration. Groundwater flowlines may converge in hillslopes of concave topography (hollows) where elevation contours bend away from the main channel of the stream, potentially causing groundwater to exfiltrate at the foot of the hillslope (Anderson and Burt, 1978; Genereux et al., 1993). If exfiltrated water ponds and re-infiltrates in the riparian area, it may follow a relatively short flowpath from there to the streambed, arriving with very young apparent age. This exfiltration and ponding was observed on the left side of Georgia Branch at GB590, on November 20, 2019, where a large pool had formed in the riparian area at the base of a hollow.

8.7. Interpretation of *TTD* mechanisms

Groundwater samples from Georgia Branch with very young apparent ages have a variety of PFAS concentrations that are probably determined by the date of initial infiltration and then groundwater recharge. The low recharge rate mechanism and re-infiltration mechanism (sections 8.5 and 8.6) seem like the most likely potential explanations for the very young apparent ages measured in the February 2019 samples. These very young apparent ages likely do not indicate the original date of PFAS deposition or initial date of recharge of this water in the surficial aquifer.

Groundwater with older apparent ages and a range of PFAS concentrations may be from areas where the re-infiltration mechanism and loss of ^{3}He at the water table are not significant factors. Such areas might occur where the shallow clay horizon and perched saturated zone are missing. Hydrostratigraphic cross-sections from Geosyntec indicate that the shallow clay causing perched saturation is absent in some areas within the Fayetteville Works (2019c, p. 212-214).

There may be a bimodal groundwater *TTD*, with a peak at 0-5 years, from groundwater affected by the low recharge rate and re-infiltration mechanisms (sections 8.5 and 8.6), and a peak at older apparent ages more typical of groundwater not affected by these two mechanisms. Georgia Branch shows this bimodal pattern with a majority of discharge consisting of groundwater with very young apparent ages (21/24 sampled points), and a minority of groundwater with older apparent ages similar to those in areas where recharge is not intercepted and rerouted to discharge by a perched saturated zone (Kennedy et al., 2009a,b; Gilmore et al., 2016a).

Using the *MTT* from the groundwater with young apparent ages may suggest a much shorter transit time for contaminated groundwater in the Georgia Branch basin than exists in reality, as much of the water may be undergoing some sort of reset to the tritium-helium age dates. The very young apparent ages might not reflect the full travel time of groundwater or PFAS through the surficial aquifer in the watershed. To understand the full travel time of PFAS through the watershed, it would be necessary to study the range of ages and travel times through the perched saturated zone and, from there, downslope to an area of re-infiltration, and to investigate further the potential for the loss of tritiogenic ^{3}He at the regional water table due to a low recharge rate.

To summarize the effects of the mechanisms which may have altered tritium-helium age dating of groundwater at Georgia Branch:

1. Sampling in the hyporheic zone
    - Water samples with young apparent ages would be mostly stream water
        - Samples with older apparent ages would be groundwater
    - Expect to see a very narrow range of PFAS concentrations clustered around the stream water concentration (Figs. 10-19)
        - Exceptions to this narrow range would be points where sampling occurred below the hyporheic zone
    - Unlikely given that all 24 points had upward water flux and the water with young apparent ages had a large range of PFAS concentrations
2. Diffusive fractionation of ^{3}He
    - Expect to have a wide range of true groundwater ages and PFAS concentrations but $^{3}H/^{3}He$ age dating would indicate very young ages
        - Except, some older apparent ages if some areas are not affected by this mechanism
    - Thought to be significant only in groundwater on the rising limb of the ^{3}H bomb peak (1950-1963), likely no groundwater this old among the Georgia Branch samples
3. The low recharge rate mechanism
    - If occurring everywhere: *TTD* would be biased toward young apparent ages
        - If it occurred only in some places: *TTD* may be bimodal (some groundwater biased young, some not)

- Expect to have a wide range of true groundwater ages and different PFAS concentrations but $^{3}H/^{3}He$ age dating would indicate very young ages
    - Except some older apparent ages if some areas are not affected by this mechanism
- Seems possible, low recharge necessary for this mechanism could occur due to the perched saturated zone

4. The re-infiltration mechanism

- Unlike the other mechanisms, the young apparent ages that occur due to this mechanism would be true groundwater ages, representative of short flowpaths from riparian area to streambed.
    - Samples with older apparent ages might not have been affected by this mechanism
- If occurring everywhere: *TTD*s for water or for PFAS do not reflect the full transit time through the watershed, only the last short subsurface flowpath from riparian area to streambed
    - If it occurred only in some places: *TTD* may be bimodal with some groundwater biased young and some not
- Groundwater may have a wide variety of flowpaths and a wide range of PFAS concentrations before exfiltration but mixing may occur during downslope flow and ponding and decrease the range of PFAS concentrations (compared to the range that might exist under the low recharge rate mechanism)

9. Summary and Conclusions

The hydrogeological conditions of Georgia Branch measured during the February 2019 sampling campaign indicate a stream with high discharge from groundwater to surface water. The coefficient of variability of PFAS flux was more similar to that of groundwater flux than to that of PFAS concentrations, suggesting that the spatial variability of groundwater flux controlled the spatial variability of PFAS flux. As the variability in groundwater flux into the stream was largely determined by variation in streambed hydraulic conductivity (Fig. 5), spatial variation in hydraulic conductivity was, therefore, an important factor in spatial variability of PFAS flux.

High PFAS concentrations were measured at all sampling points in Georgia Branch. Of the 27 PFAS measured in the Georgia Branch water samples, 8 PFAS make up 99.87% of the total measured PFAS concentrations at all sampling points (PMPA at 37.9%, GenX at 23.4%, PFO2HxA at 16.7%, PEPA at 13.6%, Nafion Bp 4 at 3.10%, PFMOAA at 2.56%, PFO3OA at 2.02%, and Nafion Bp 2 at 0.482%). The average GenX concentration of groundwater samples was 477 ng L^{-1} and only 4 of the 24 sampling points had concentrations below the state recommended drinking water health goal for GenX of 140 ng L^{-1}. Using the measurements from February 2019, an estimated 67.9 g of PFAS was discharged from groundwater into Georgia Branch and its tributaries per day. This contaminated water then flows into the Cape Fear River from where it may enter water systems downstream.

Tritium-helium age dating of streambed groundwater suggested that the groundwater discharging into Georgia Branch had predominantly very young apparent ages (0-5 years). Only 3 out of 24 samples were groundwater with older apparent ages (about 14, 18, and 28 years). The groundwater at GB412R ($^{3}H/^{3}He$ age = 28 years), considering its high ^{4}He concentrations and

low R/R_a value, may represent a mixture of 28-year-old groundwater with much older groundwater that was recharged to the aquifer some years before PFAS contamination occurred. The range found at of ages Georgia Branch was unexpected and significantly different from what other datasets collected with the same general approach have found [e.g., Browne and Guldan, 2005; Kennedy et al., 2009a,b; Gilmore et al., 2016a].

While a wide range of PFAS concentrations was measured among the groundwater samples from Georgia Branch, a general pattern of decreasing concentration with increasing age was observed (Figs. 10-19). Although retardation of chemicals in an aquifer may affect individual transit time, the retardation factors of the most abundant PFAS found in Georgia Branch groundwater are similar and close to 1. These retardation factors suggest that the more important factor in transit time through the surficial aquifer is the history of emissions of each PFAS.

Groundwater with very low to no PFAS concentration in the Georgia Branch basin likely indicates groundwater older than 48 years, since the Fayetteville Works was built in 1971 and so could not have emitted PFAS for longer than 48 years. No groundwater samples without PFAS have been found in the Georgia Branch basin, during the February 2019 sampling campaign or previously (Koropeckyj-Cox, 2019). The lack of PFAS-free groundwater in this study, in combination with observations from previous work on groundwater PFAS at the site (Koropeckyj-Cox, 2019), suggests that the *MTT* of groundwater through the surficial aquifer may be relatively short, roughly two decades.

Two hydrogeological mechanisms are hypothesized to have been significant enough at the site to affect the unexpected distribution of apparent groundwater ages. The lack of retention of ^3He at the water table due to low recharge rates would represent a basic limitation on the

applicability of tritium-helium age dating at Georgia Branch. If this mechanism occurs, it suggests that the *TTD* from Georgia Branch in February 2019 is biased toward young apparent ages. If the re-infiltration mechanism were the main mechanism affecting the apparent age of groundwater discharging to Georgia Branch, then the ages generated may be accurate groundwater ages that represent only the very short flow path from the riparian area to the streambed and not the previous longer flow path through the surficial aquifer from initial recharge.

9.1. Future Work

Further research is necessary to understand which of the identified mechanisms are affecting tritium-helium age dating of groundwater at Georgia Branch. A different age dating method could possibly shed light on the reason for so many very young $^{3}H/^{3}He$ apparent ages, and provide more information on groundwater age. Gas exchange at the water table due to low recharge rates may be alleviated by using an age dating method relying on chemicals with lower diffusion coefficients, such as sulfur hexafluoride (SF_6) age dating. SF_6 is a stable atmospheric gas of primarily anthropogenic origin, with a low molecular diffusion coefficient, that is used in groundwater age dating (Busenberg and Plummer, 2000). SF_6 may be slower to equilibrate with the atmosphere than ^{3}He during downslope flow after exfiltration, and thus possibly less likely than helium to be affected by the low recharge rate or re-infiltration mechanisms. Between the two mechanisms, the re-infiltration mechanism may be more likely to result in similar SF_6 and $^{3}H/^{3}He$ dates; exfiltrated water flowing downslope in small rivulets seems likely to equilibrate with the atmosphere fairly quickly, perhaps before re-infiltration in the riparian area.

The diffusion coefficient of SF_6 in water ($9.46x10^{-6}$ cm^2 s^{-1}) (King and Saltzman, 1995) is about 5.8 times smaller than that of ^3He ($5.5x10^{-5}$ cm^2 s^{-1}) (Wise and Houghton, 1996). This lower diffusion coefficient could mitigate the loss of the measured compound at the water table from low recharge rates. Finding groundwater with older apparent SF_6 ages at the same points sampled in Georgia Branch in February 2019 may suggest that the young apparent $^3H/^3He$ ages were due to lack of retention of ^3He at the water table due to low recharge rate.

If the re-infiltration mechanism were a major factor at Georgia Branch, and if water was fully re-equilibrated with the atmosphere before re-infiltration, then SF_6 age dating results should be similar to the tritium-helium age dating results. If SF_6 in the re-infiltrated water had not been exposed to the atmosphere for long enough to fully re-equilibrate, then older ages may be found. Nevertheless, similar ages when comparing the age dating results from $^3H/^3He$ and SF_6 at the same points may favor the re-infiltration mechanism over the lack of retention of ^3He at the water table, since it seems likely that downslope surface flow following exfiltration from the perched saturated zone could lead to atmospheric equilibration for the water involved, even for a gas like SF_6 with a smaller diffusion coefficient.

Stream water collected 16 January 2020 in Georgia Branch appears to have non-zero age based on SF_6: 4 years at GB100, 10 years at GB585 (pers. comm., D.P. Genereux, 2020). In other words, stream water at GB585 had an older age date by SF_6 than most of the streambed groundwater did by tritium-helium age dating. These ages seem consistent with the low recharge rate mechanism where SF_6 would be less affected than ^3He by gas exchange at the water table. These results may be consistent with the re-infiltration mechanism, as well, if water does not re-equilibrate with the atmosphere with respect to SF_6 during downslope flow (i.e., if the SF_6 "clock" is not completely reset prior to re-infiltration in the riparian area).

REFERENCES

Abbott, L.E., K.M.J. Farrell, J.G. Nickerson, and N.K Gay (2011), "Lithic resources of the North Carolina Coastal Plain: prehistoric acquisition and utilization patterns." The Archaeology of North Carolina: Three Archaeological Symposia. *North Carolina: North Carolina Archaeological Council Publication*. No. 30.

Aeschbach-Hertig, W., D. K. Solomon (2013), Noble gas thermometry in groundwater hydrology, in *The Noble Gases as Geochemical Tracers*, edited by P. Burnard, pp. 81–122.

Anderson, M.G., T.P. Burt (1978), The role of topography in controlling throughflow generation, *Earth Surface Processes*, 3(1978), 331-344. doi: 10.1002/esp.3290030402

Bao, Y., S. Deng, X. Jiang, Y. Qu, Y. He, L. Liu, Q. Chai, M. Mumtaz, J. Huang, G. Cagnetta, G. Yu (2018), Degradation of PFOA Substitute: GenX (HFPO-DA Ammonium Salt): Oxidation with UV/Persulfate or reduction with UV/Sulfite? *Environmental Science Technology,* 52(20): 11728-11734. doi:10.1021/acs.est.8b02172.

Browne, B. A., and N. M. Guldan (2005), Understanding long-term baseflow water quality trends using a synoptic survey of the ground water-surface water interface, Central Wisconsin, *Journal of Environmental Quality*, 34(3), 825–835.

Buck, R. C., J. Franklin, U. Berger, J.M. Conder, I.T. Cousins, P. de Voogt, A.A. Jensen, K. Kannan, S.A. Mabury, S.P.J van Leeuwen (2011), Perfluoroalkyl and polyfluoroalkyl substances in the environment: Terminology, classification, and origins. *Integrated Environmental Assessment and Management*, 7(4), 513−541.

Busenberg, E., L.N. Plummer (2000), Dating young groundwater with sulfur hexafluoaride: Natural and anthropogenic sources of sulfur hexafluoride. Water Resources Research, 36(10), 3011-3030. doi: 10.1029/2000WR900151

DuPont, E.I., Fayetteville Works (2002) [Hazardous waste documentation, File ID: 29235], Draft RCRA Phase I Work Plan, North Carolina Department of Environmental Quality Waste Management Online Documents (Program ID: NCD047368642).

DuPont, E.I., Fayetteville Works (1980) [Site photos and map, File ID:1358591], Correspondence, North Carolina Department of Environmental Quality Waste Management Online Documents (Program ID: NCD047368642).

Gebbink W.A., L. van Asseldonk, S.P.J. van Leeuwen (2017), Presence of emerging per- and polyfluoroalkyl substances (PFASs) in river and drinking water near a fluorochemical production plant in the Netherlands. *Environmental Science Technology,* 51(19), 11057-11065. doi:10.1021/acs.est.7b02488.

Genereux, D.P., H.F. Hemond, P.J. Mulholland (1993) Spatial and temporal variability in streamflow generation on the West Fork of Walker Branch Watershed. *Journal of Hydrology*. 142(1-4), 137-166. doi: 10.1016/0022-1694(93)90009-X

Genereux, D.P., S. Leahy, H. Mitasova, C.D. Kennedy, D.R. Corbett (2008), Spatial and temporal variability of streambed hydraulic conductivity in West Bear Creek, North Carolina, USA. *Journal of Hydrology*, 358(3-4), 332-353. doi:10.1016/j.jhydrol.2008.06.017

Geosyntec Consultants of North Carolina, Inc. (Geosyntec) (2019a) Corrective Action Plan: Chemours Fayetteville Works. *Report, prepared for The Chemours Company*. Project Number TR0795.

Geosyntec Consultants of North Carolina, Inc. (Geosyntec) (2019b) Corrective Action Plan: Appendix C: K_{ow}, K_{oc}, and Mass Distribution Calculations. *Report, prepared for The Chemours Company*. Project Number TR0795. https://deq.nc.gov/news/key-issues/genx-investigation/chemours-consent-order-february-2019.

Giese, G.I., J.L. Eimers, and R.W. Coble (1997), Simulation of ground-water flow in the Coastal Plain aquifer system of North Carolina. United States Geological Survey, 1-142.

Gilmore, T. E., D. P. Genereux, D. K. Solomon, and J. E. Solder (2016a), Groundwater transit time distribution and mean from streambed sampling in an agricultural coastal plain watershed, North Carolina, USA, *Water Resources Research*, 52, 2025–2044, doi:10.1002/2015WR017600.

Gilmore, T. E., D. P. Genereux, D. K. Solomon, K. M. Farrell, and H. Mitasova (2016b), Quantifying an aquifer nitrate budget and future nitrate discharge using field data from streambeds and well nests. *Water Resources Research*, *52*(11), 9046-9065, doi: 10.1002/2016WR018976.

Gilmore, T.E., D.P. Genereux, D.K. Solomon, J.E. Solder, B.A. Kimball, H. Mitasova, F. Birgand (2016c) Quantifying the fate of agricultural nitrogen in an unconfined aquifer: stream-based observations at three measurement scales. *Water Resources Research*, 52, 1961-1983. doi:10.1002/2015WR017599

Hopkins, Z.R., M. Sun, J.C. DeWitt, and D.R. Knappe (2018), Recently Detected Drinking Water Contaminants: GenX and Other Per-and Polyfluoroalkyl Ether Acids. *Journal-American Water Works Association* 110, 13-28.

Hvorslev, M. J. (1951), Time lag and soil permeability in groundwater observations, *U. S. Army Bulletin 36*, Waterways Exp. Station, Corps of Eng., Vicksburg, Miss.

Kennedy, C.D., D.P. Genereux (2007) ^{14}C groundwater age and the importance of chemical fluxes across aquifer boundaries in the confined Cretaceous aquifers of North Carolina, USA. *Radiocarbon*, 49(30), 1181-1203.

Kennedy, C.D., D.P. Genereux, D.R. Corbett, and H. Mitasova (2007), Design of a light-oil piezomanometer for measurement of hydraulic head differences and collection of groundwater samples. *Water Resources Research*, 43, W09501, doi:10.1029/2007WR005904.

Kennedy, C.D., D.P. Genereux, D.R. Corbett, and H. Mitasova (2009a), Relationships among groundwater age, denitrification, and the coupled groundwater and nitrogen fluxes through a streambed. *Water Resources Research*, 45, W09402. doi 10.1029/2008WR007400

Kennedy, C.D., D.P. Genereux, D.R. Corbett, and H. Mitasova (2009b), Spatial and temporal dynamics of coupled groundwater and nitrogen fluxes through a streambed in an agricultural watershed. *Water Resources Research*, 45, W09401. doi 10.1029/2008WR007397

King, D.B., E.S. Saltzman (1995), Measurement of the diffusion coefficient of sulfur hexafluoride in water. Journal of Geophysical Research, 100(C4), 7083-7088. doi: 10.1029/94JC03313

Koropeckyj-Cox, L. (2019), Quantifying the transport of per- and polyfluoroalkyl substances (PFAS) from groundwater to surface water near the Chemours property in Bladen County, NC. (Master's thesis). North Carolina State University, Raleigh, North Carolina.

LaBolle, E. M., G. E. Fogg, and J. B. Eweis (2006), Diffusive fractionation of ^{3}H and ^{3}He in groundwater and its impact on groundwater age estimates, *Water Resources Research*, 42, W07202, doi:10.1029/2005WR004756.

Lindsey, B. D., S. W. Phillips, C. A. Donnelly, G. K. Speiran, L. N. Plummer, J. K. Bohlke, M. J. Focazio, W. C. Burton, and E. Busenberg (2003), Residence times and nitrate transport in ground water discharging to streams in the Chesapeake Bay watershed. *Water Resources Investigations Report 03-4035,* U.S. Geologic Survey, Reston, Va.

Nickels, J.L. (2016), Coupled Groundwater and Volatile Organic Compound Fluxes through a Coastal Plain Streambed, North Carolina. (Master's thesis). North Carolina State University, Raleigh, North Carolina.

North Carolina Climate Office (NC Climate) 2012, Southeast Temperature. North Carolina State University. https://climate.ncsu.edu/edu/SETemp

North Carolina Department of Environmental Quality (NCDEQ) (2017a) "State orders Chemoursto stop chemical releases, begins legal action and steps to suspend permit." North Carolina Department of Environmental Quality, https://deq.nc.gov/state-orders-chemours-stop-chemical-releases-begins-legal-action-and-steps-suspend-permit.

North Carolina Department of Environmental Quality (NCDEQ) (2018) "Rainwater Sampling." GenX Investigation: Air Quality Sampling, NC DEQ. https://deq.nc.gov/news/key-issues/genx-investigation/air-quality-sampling

North Carolina Department of Environmental Quality (NCDEQ) (2019a) "Hydrogeology: hydrogeologic framework database access." Division of Water Resources, NCDEQ. https://www.ncwater.org/?page=348.

North Carolina Department of Environmental Quality (NCDEQ) (2019b) "Water Resources Data: Ground Water Levels." Division of Water Resources, NC DEQ. https://www.ncwater.org/?page=343.

North Carolina Department of Environmental Quality (NCDEQ) (2019c) "Signed Consent Order February 26, 2019." GenX Investigation, NC DEQ. https://deq.nc.gov/news/key-issues/genx-investigation/chemours-consent-order-february-2019

Poreda, R. J., T.E. Cerling, D.K. Solomon (1988) "Tritium and helium isotopes as hydrologic tracers in a shallow unconfined aquifer." *Journal of Hydrology*, 103(1-2), 1-9, doi:10.1016/0022-1694(88)90002-9.

Schlosser, P., M. Stute, H. Dörr, C. Sonntag, and K. O. Münnich (1988), Tritium/^{3}He dating of shallow groundwater, *Earth and Planetary Science Letters*, 89(3–4), 353–362, doi:10.1016/0012-821X(88)90122-7.

Schlosser, P., M. Stute, C. Sonntag, K. O. Münnich (1989), Tritiogenic ^{3}He in shallow groundwater, *Earth and Planetary Science Letters*, 94(3-4), 245-256, doi: 10.1016/0012-821X(89)90144-1

Solomon, D.K., and P.G. Cook (2000), "^{3}H and ^{3}He" in *Environmental Tracers in Subsurface Hydrology*, edited by P.G. Cook and A. Herczeg, 397-424, Kluwer Academic, Boston, Mass.

Solomon, D.K., D.P. Genereux, L.N. Plummer, E. Busenberg (2010), Testing mixing models of old and young groundwater in a tropical lowland rain forest with environmental tracers, *Water Resources Research*, 46, W04518. doi:10.1029/2009WR008341

Solomon, D.K., A. Hunt, R.J. Poreda (1996), Source of radiogenic helium 4 in shallow aquifers: Implications for dating young groundwater. *Water Resources Research.*, 32(6), 1805-1813. doi: 10.1029/96WR00600

Solomon, D.K., R.J. Poreda, S.L. Schiff, J.A. Cherry (1992), Tritium and Helium 3 as Groundwater Age Tracers in the Borden Aquifer. *Water Resources Research*, 28(3), 741-755. doi:10.1029/91WR02689.

Strynar, M., S. Dagnino, R. McMahen, S. Liang, A. Lindstrom, E. Anderson, L. McMillan, M. Thurman, I. Ferrer, C. Ball (2015), Identification of Novel Perfluoroalkyl Ether Carboxylic Acids (PFECAs) and Sulfonic Acids (PFESAs) in Natural Waters Using Accurate Mass Time-of-Flight Mass Spectrometry (TOFMS). *Environmental Science & Technology*, 49(19), 11622-11630. doi: /10.1021/acs.est.5b01215

Sun, M., E. Arevalo, M. Strynar, A. Lindstrom, M. Richardson, B. Kearns, A. Pickett, C. Smith, and D.R.U. Knappe (2016), Legacy and Emerging Perfluoroalkyl Substances Are Important Drinking Water Contaminants in the Cape Fear River Watershed of North Carolina. *Environmental Science & Technology Letters* 3, 415-419. doi: 10.1021/acs.estlett.6b00398.

United States Environmental Protection Agency (US EPA), 2016. Fact Sheet: PFOA & PFOS Drinking Water Health Advisories. United States Environmental Protection Agency.

United States Environmental Protection Agency (Comptox) (2019), Comptox Chemistry Dashboard. https://comptox.epa.gov/dashboard

U.S. Geological Survey, National Geospatial Technical Operations Center (USGS Map) (2016a) USGS Combined Vector for Ammon, North Carolina 20160706 7.5 x 7.5 minute Shapefile: U.S. Geological Survey.

U.S. Geological Survey, National Geospatial Technical Operations Center (USGS Map) (2016b) USGS Combined Vector for Autryville, North Carolina 20160712 7.5 x 7.5 minute Shapefile: U.S. Geological Survey.

U.S. Geological Survey, National Geospatial Technical Operations Center (USGS Map) (2016c) USGS Combined Vector for Cedar Creek, North Carolina 20160618 7.5 x 7.5 minute Shapefile: U.S. Geological Survey.

U.S. Geological Survey, National Geospatial Technical Operations Center (USGS Map) (2016d) USGS Combined Vector for Duart, North Carolina 20160707 7.5 x 7.5 minute Shapefile: U.S. Geological Survey.

U.S. Geological Survey, National Geospatial Technical Operations Center (USGS Map) (2016e) USGS Combined Vector for Dublin, North Carolina 20160618 7.5 x 7.5 minute Shapefile: U.S. Geological Survey.

U.S. Geological Survey, National Geospatial Technical Operations Center (USGS Map) (2016f) USGS Combined Vector for Elizabethtown North, North Carolina 20160618 7.5 x 7.5 minute Shapefile: U.S. Geological Survey.

U.S. Geological Survey, National Geospatial Technical Operations Center (USGS Map) (2016g) USGS Combined Vector for Hope Mills, North Carolina 20160712 7.5 x 7.5 minute Shapefile: U.S. Geological Survey.

U.S. Geological Survey, National Geospatial Technical Operations Center (USGS Map) (2016h) USGS Combined Vector for Jerome, North Carolina 20160712 7.5 x 7.5 minute Shapefile: U.S. Geological Survey.

U.S. Geological Survey, National Geospatial Technical Operations Center (USGS Map) (2016i) USGS Combined Vector for Northeast Lumberton, North Carolina 20160713 7.5 x 7.5 minute Shapefile: U.S. Geological Survey.

U.S. Geological Survey, National Geospatial Technical Operations Center (USGS Map) (2016j) USGS Combined Vector for Roseboro, North Carolina 20160618 7.5 x 7.5 minute Shapefile: U.S. Geological Survey.

U.S. Geological Survey, National Geospatial Technical Operations Center (USGS Map) (2016k) USGS Combined Vector for Saint Pauls, North Carolina 20160618 7.5 x 7.5 minute Shapefile: U.S. Geological Survey.

U.S. Geological Survey, National Geospatial Technical Operations Center (USGS Map) (2016l) USGS Combined Vector for Tar Heel, North Carolina 20160711 7.5 x 7.5 minute Shapefile: U.S. Geological Survey.

U.S. Geological Survey (USGS Map) (2017) The National Map. 3DEP products and services: The National Map, 3D Elevation Program. Web page, accessed April 2019 at https://nationalmap.gov/3DEP/3dep_prodserv.html.

U.S. Geological Survey (USGS) (2005), Coastal Plain Ground-Water Recharge. South Atlantic Water Science Center – North Carolina Office. Web page, accessed April 2020 at https://nc.water.usgs.gov/projects/coastal_gw/index.html.

US Climate Data (2019) "Fayetteville Weather Averages." Climate Fayetteville - North Carolina and Weather Averages Fayetteville, www.usclimatedata.com/climate/fayetteville/north-carolina/united-states/usnc1259.

Wang, Z., J.C. DeWitt, C.P. Higgins, and I.T. Cousins (2017), A Never-Ending Story of Per- and Polyfluoroalkyl Substances (PFASs)? *Environmental Science & Technology.* 51(5): 2508-2518.

Winner Jr, M.D., and R.W. Coble (1989), Hydrogeologic framework of the North Carolina Coastal Plain aquifer system. United States Geological Survey, 1-119.

Wise, D.L. and G. Houghton (1966), The diffusion coefficients of ten slightly soluble gases in water at 10-60°C. *Chemical Engineering Science*, 21, 999-1010. doi: 1 0.1016/0009-2509(66)85096-0

Xiao, F. (2017) Emerging poly- and perfluoroalkyl substances in the aquatic environment: A review of current literature. *Water Research*, 124, 482-495. doi: 10.1016/j.watres.2017.07.024

APPENDIX

Appendix A. Tritium-Helium Age Dating Results and Noble Gas Analysis

Table A1. Tritium-helium age dating analysis and noble gas analysis as prepared by D. K. Solomon's laboratory at the University of Utah. The concentration of tritium (^3H) is listed in tritium units (1 TU = 3.22 picocuries per liter) and the standard deviation, or one sigma, for the tritium content is in TU, as well. R/R_a, where R is $[^3He]/[^4He]$ in the groundwater sample and R_a is the atmospheric $[^3He]/[^4He]$, has no units. The total concentration of helium, helium-3, and helium-4 are measured in cm^3 STP g^{-1} of water. Age is listed in year and calculated using the International Atomic Energy Agency's iNOBLE v.2.2 closed-system equilibration (CE) model. Total concentrations of Ne, Ar, Kr, and Xe were measured in cm^3 STP per liter. The deviation of the measured neon concentration from saturation at the estimated recharge temperature, ΔNe, is calculated as $\left(\frac{[Ne]_{measured}}{[Ne]_{equilibrium}} - 1\right) * 100$, a positive value indicates the presence of excess air.

Table A1.

Sampling Point	[Tritium] (TU)	Sigma Error (TU)	R/R_a	[Total He] (cc STP g^{-1} water)	[^{3}He] (cc STP g^{-1} water)	[^{4}He] (cc STP g^{-1} water)	Age (yr)
GB20R	3.92	0.66	0.978	3.32E-08	4.50E-14	3.32E-08	**0**
GB50C	3.06	0.23	1.11	5.36E-08	8.26E-14	5.36E-08	**14**
GB90L	4.37	0.56	0.957	5.16E-08	6.83E-14	5.16E-08	**0**
GB130C	3.75	0.47	0.995	5.27E-08	7.25E-14	5.27E-08	**0.7**
GB170L	4.06	0.31	0.981	3.76E-08	5.11E-14	3.76E-08	**0**
GB210C	4.56	0.39	1.00	5.09E-08	7.06E-14	5.09E-08	**1.2**
GB250R	3.41	0.43	1.01	4.70E-08	6.54E-14	4.70E-08	**2.4**
GB290C	3.74	0.47	1.02	3.35E-08	4.71E-14	3.35E-08	**2.8**
GB330L	3.27	0.42	0.930	5.27E-08	6.79E-14	5.27E-08	**0**
GB330C	3.61	0.46	0.970	4.15E-08	5.57E-14	4.15E-08	**0**
GB330R	3.96	0.52	0.975	2.54E-08	3.43E-14	2.54E-08	**0**
GB387L	4.68	0.44	1.00	4.72E-08	6.54E-14	4.72E-08	**0.9**
GB387C	4.72	0.45	0.975	4.23E-08	5.71E-14	4.23E-08	**0**
GB387R	3.44	0.76	0.944	4.15E-07	5.42E-13	4.15E-07	**0**
GB412L	3.54	0.69	0.975	4.46E-08	6.02E-14	4.46E-08	**0**
GB412C	3.69	0.49	1.01	4.32E-08	6.01E-14	4.32E-08	**2.9**
GB412R	2.23	0.23	0.748	9.40E-08	9.73E-14	9.40E-08	**28**
GB450L	3.34	0.41	1.00	2.77E-08	3.84E-14	2.77E-08	**1.5**
GB450C	3.87	0.38	0.969	4.69E-08	6.30E-14	4.69E-08	**0**
GB450R	3.93	0.50	0.962	4.65E-08	6.19E-14	4.65E-08	**0**
GB487L	2.11	0.18	1.01	4.88E-08	6.83E-14	4.88E-08	**4.7**
GB490C	3.16	0.42	1.15	5.02E-08	7.96E-14	5.02E-08	**18**
GB490R	2.91	0.37	0.950	4.75E-08	6.24E-14	4.75E-08	**0**
GB530C	3.53	0.44	0.970	4.72E-08	6.34E-14	4.72E-08	**0**

Table A1 (continued).

Sampling Point	[Total Ne] (cc STP g^{-1} water)	[Total Ar] (cc STP g^{-1} water)	[Total Kr] (cc STP g^{-1} water)	[Total Xe] (cc STP g^{-1} water)	Δ Ne
GB20R	1.49E-07	2.67E-04	5.96E-08	8.57E-09	-14.1
GB50C	2.25E-07	3.62E-04	7.53E-08	1.10E-08	18.8
GB90L	2.29E-07	3.73E-04	7.85E-08	1.10E-08	21.1
GB130C	2.22E-07	3.52E-04	8.30E-08	1.16E-08	14.8
GB170L	1.65E-07	2.86E-04	5.78E-08	8.19E-09	-6.27
GB210C	2.25E-07	3.50E-04	7.99E-08	1.09E-08	17.8
GB250R	2.29E-07	3.92E-04	8.22E-08	1.21E-08	17.0
GB290C	1.47E-07	2.91E-04	6.26E-08	6.37E-09	-13.9
GB330L	2.08E-07	3.51E-04	7.31E-08	1.10E-08	9.56
GB330C	1.98E-07	3.59E-04	7.57E-08	1.17E-08	2.62
GB330R	1.10E-07	2.11E-04	4.59E-08	7.25E-09	-29.3
GB387L	2.21E-07	3.48E-04	7.11E-08	2.07E-09	19.1
GB387C	1.85E-07	3.08E-04	6.50E-08	9.18E-09	2.36
GB387R	2.17E-06	1.20E-03	1.53E-07	1.71E-08	1207
GB412L	2.06E-07	3.77E-04	8.03E-08	1.20E-08	5.66
GB412C	1.44E-07	2.30E-04	4.72E-08	7.00E-09	-12.8
GB412R	2.23E-07	3.36E-04	7.35E-08	1.08E-08	18.8
GB450L	1.19E-07	1.98E-04	4.18E-08	5.86E-09	-22.8
GB450C	2.15E-07	3.69E-04	8.16E-08	1.19E-08	10.6
GB450R	2.11E-07	3.78E-04	8.56E-08	1.26E-08	6.57
GB487L	2.28E-07	3.93E-04	8.26E-08	1.19E-08	17.8
GB490C	1.98E-07	3.09E-04	6.69E-08	9.92E-09	7.48
GB490R	2.21E-07	3.80E-04	8.00E-08	1.17E-08	14.8
GB530C	2.13E-07	3.91E-04	8.44E-08	1.29E-08	7.41